Chapter 13

Photobioreactors Design for Hydrogen Production

José Maria Fernández-Sevilla,
Francisco Gabriel Acién-Fernández, and Emilio Molina-Grima*
Department of Chemical Engineering, University of Almería,
Almería 04071, Spain

Summary

The photobiological production of H_2 is a subject that has been studied with great intensity over the past 50 years using different approaches; direct or indirect biophotolysis (green algae and cyanobacteria) and photo-fermentations (photosynthetic bacteria). The number of publications on the subject is impressive. However, hardly any of the production methods proposed have progressed beyond the laboratory, and the photobioreactors (PBR) used to carry out the processes are still bench-top scale laboratory devices. The scale up of some of the proposed PBR to carry out the process outdoor using full solar radiation is just beginning and the existing data are too scarce.

This chapter is mainly addressing the major issues in the design and scale up of photobioreactors (PBR) for the eventual photobiological production of H_2 when using an envisaged two-stage scheme. A first one in which microalgae are cultivated in large open ponds to produce microalgae biomass with a high C/N ratio; then, by changing the physiological conditions, a second anoxygenic step to produce hydrogen in closed PBRs. The different

*Author for correspondence, e-mail: emolina@ual.es

D. Zannoni and R. De Philippis (eds.), Microbial BioEnergy: Hydrogen Production,
Advances in Photosynthesis and Respiration 38, pp. 291–320, DOI 10.1007/978-94-017-8554-9_13,

designs currently used for practical microalgae mass culture are reviewed, identifying their characteristic parameters. The major operational variables impacting on PBR performances are also highlighted, as well as the challenges associated with the PBR design and scale up. Finally, the bottlenecks for the scaling up of the different technologies and thus of the photobiological H_2 production are discussed.

I. Introduction

The current hydrogen production is based on thermochemical processes (mainly steam reforming of methane) that use fossil fuel, thus being great producers of CO_2. Only a small fraction of current world production comes from water electrolysis (Berberoglu et al. 2008). This latter approach would be even more sustainable if the electricity required for electrolysis came from photovoltaic cells. However, this technology is quite expensive and the cost remains a major drawback. Therefore, the world's growing energy needs will place much greater reliance on a combination of fossil fuel-free energy sources and new technologies for capturing sunlight and converting atmospheric CO_2. Within these technologies falls the photosynthetic hydrogen production from sunlight and water with the possible advantage of CO_2 capture, which has been investigated with great dedication over the past 50 years (Levin et al. 2004; Laurinavichene et al. 2006; Das and Veziroglu 2008). The advantages most highlighted in these studies, with respect to the current industrial technologies for producing H_2 are: (a) the biological H_2 production occurs under mild temperature and pressure conditions, (b) the reaction specificity is typically higher than that of inorganic catalysts used in thermochemical processes and (c) there is a diverse collection of raw materials, including waste, that can serve as feedstock for the production of photobiological H_2.

In theory, the photobiological production of hydrogen from water requires an efficient microalgae capable of converting protons to H_2 and low cost PBRs. The selected microalgal strains should exhibit a high hydrogen production rate and high light to hydrogen conversion efficiencies when using dense cultures outdoors (Benemann 1997, 2000). The PBRs must expose the H_2-producing cultures to sunlight and at the same time allow the recovery of the gas produced (Berberoglu et al. 2008). Most of the studies on photobiological H_2 production so far available have been carried out in well-equipped lab scale photobioreactors having various geometries (Levin et al. 2004; Berberoglu et al. 2008; Oncel and Sabankay 2012). In addition, due to differences in (i) the design of the PBRs, (ii) the light sources, (iii) the temperature of operation, (iv) the microorganism used and (v) the media used, the results reported in the literature for H_2 production show large variations of over a hundred fold (Eroglu and Melis 2011). For example: the maximum reported H_2 production rate for *C. reinhardtii* outdoors was 0.61 ml L^{-1} h^{-1} in a process which used a second phase with sulphur deprivation to induce H_2 production (Giannelli and Torzillo 2012). However, for the cyanobacterium *Anabaena variabilis,* some of the reported data are: 167.6 mmol H_2 g chl a^{-1} h^{-1} in a process using indirect biophotolysis (Sveshnikov et al. 1997); or the 150 mmol H_2 g chl a^{-1} h^{-1} reported for the marine green algae *Scenedesmus obliquus* (Florin et al. 2001). In contrast, the maximum reported H_2 production rates when using purple-non sulphur (PNS) bacteria in a outdoor photofermentative process was 27.2 ml L^{-1} h^{-1} by using a horizontal tubular PBR (Adessi et al. 2012), and 5.9 mol H_2 kg^{-1} h^{-1} for *Rhodobacter spharoides* (Sasikala et al. 1991).

Although some advances have been recently made, there are still many prob-

lems in the different routes proposed that should have to be solved before a practical photobiological production process could be set up. The major drawbacks so far reported are related to the very low yields attained, well below those achievable for the production of other biofuels from the same feedstocks (Hallenbeck and Benemann 2002). Moreover, low yields may also lead to the generation of side products which being produced in large volumes, would generate a significant disposal problem. On the other hand, another major challenge when scaling up the photobiological H_2 production, is connected with the use of economically viable PBRs, and the sparse data available on outdoor production of H_2 using a fully sealed PBR (Hallenbeck et al. 2012).

II. Major Routes for the Photobiological H_2 Production

There are several pathways for photobiological hydrogen production (note that dark fermentation for producing H_2 is not addressed in this chapter). Photobiological production of H_2 includes three distinct routes such as (1) direct biophotolysis, (2) indirect biophotolysis and (3) photo-fermentation. It is also possible to design integrated systems incorporating both photosynthetic and fermentative processes (Levin et al. 2004).

Direct Biophotolysis. When microalgae use this pathway, the energy source is the sunlight in the spectral range from 400–700 nm. The catalyst producing hydrogen is the enzyme hydrogenase, extremely sensitive to oxygen. This mechanism can be considered to be the photobiological electrolysis of water and it is, theoretically, the most energy efficient for H_2 production (Prince and Kheshgi 2005). However, the oxygen produced during water splitting, irreversibly inhibits the functioning of the [Fe-Fe]-hydrogenase and the practical light-to-hydrogen conversion efficiency at full solar radiation is well below 0.1 %. This makes the process impractical for industrial applications (Hallenbeck and Benemann 2002). Green algae such as *Chlamydomonas reinhardtii*, *Scenedesmus obliquus*, and *Chlorococcum littorale* are capable of producing H_2 via direct biophotolysis (Das and Veziroglu 2001) with H_2 production rates varying between 2.5 and 13 ml of H_2 L^{-1} h^{-1} (Tsygankov et al. 1998; Laurinavichene et al. 2006).

Indirect Biophotolysis. In this mechanism, the source of electrons is also water. The electrons are first used to reduce CO_2 to form organic compounds during photosynthesis and O_2 is simultaneously generated and released. Then, in a second step, that can be carried out in the same reactor if it is closed or in another closed reactor if the first step was carried out in an open reactor, electrons are recovered from the oxidation of the organic compounds and used in generating H_2 through the action of nitrogenase (Hallenbeck and Benemann 2002). Thus, no O_2 is generated during H_2 production. Cyanobacteria such as *Anabaena variabilis*, are capable of indirect biophotolysis (Sveshnikov et al. 1997; Tsygankov et al. 1999; Pinto et al. 2002). The maximum theoretical light to H_2 energy conversion efficiency of indirect biophotolysis is about 60 % lower than that of direct biophotolysis (Prince and Kheshgi 2005) due to the fact that (i) multiple steps are involved in converting solar energy to H_2 and (ii) the use of nitrogenase enzyme requires ATP. However, the problems associated to O_2 that happen in direct biophotolysis make its actual efficiency lower than in the indirect biophotolysis. Production rates of 12.5 ml kg dry $cells^{-1}$ h^{-1} were obtained (Markov et al. 1997) by using a partial vacuum in the second step; similar to those achieved by Tsygankov et al. (2002). Yoon et al. (2006) incorporated nitrate to the culture medium to enhance the biomass productivity of *Anabaena* in the first step and increased the H_2 production rate in the second step. The authors reported maximum specific H_2 production rates of 4.1 and 0.45 L kg dry $cells^{-1}$ h^{-1} for flat panel reactors of 2 and 4 cm thick respectively. They flushed with argon in order to force the removal of the dissolved H_2 and to increase the H_2 production in the second step, as an alternative to the partial

vacuum used by Markov et al. (1997). Even higher productivities were obtained by Berberoglu et al. (2008): 5.6 L kg dry cells^{-1} h^{-1}, at 1 atm and 30 °C, when using Allen-Arnon medium in comparison with those achieved when using BG 11 medium (1 L kg dry cells^{-1} h^{-1}). However again, the reality is that the conversion efficiencies achieved by indirect biophotolysis are also below 1 %.

Photo-Fermentation. This mechanism is similar to indirect biophotolysis with the distinction that the organic compounds used are produced outside the cells via the photosynthesis of other organisms. These extracellular organic materials, such as organic acids, carbohydrates, starch, and cellulose (Kapdan and Kargi 2006), are used as electron source and sunlight is used as energy source to produce H_2 by the enzyme nitrogenase (Das and Veziroglu 2001). Since this enzyme is repressed by nitrogen fixation, photofermentation needs a high C/N ratio biomass. Since cells do not carry out oxygenic photosynthesis, no O_2 is generated and all the solar energy can be used to produce H_2. Thus, this mechanism is viewed as the most promising microbial system to produce H_2 (Das and Veziroglu 2001). The major advantages of this route are (i) the absence of O_2 evolution, which inhibits the H_2-producing enzymes, and (ii) the ability to consume a wide variety of organic substrates found in waste waters. Due to their ability to harvest a wider light spectrum, from 300 to 1,000 nm, Purple non-sulphur (PNS) bacteria such as *Rhodobacter sphaeroides, Rhodobacter capsulatus* and *Rhodopseudomonas palustris* hold promise as photo-fermentative H_2 producers (Sasikala et al. 1991; Das and Veziroglu 2001; Adessi et al. 2012).

As stated before, the [Fe-Fe] hydrogenase involved in H_2 generation during biophotolysis is irreversibly inactivated by the O_2 produced during water splitting. A milestone in solving this problem when using the green algae *C. reinhardtii* was achieved by Melis and co-workers in 2000. The key of this process lies on the second phase of microalgae growth in which Photosystem II (PSII), that plays a vital role in oxygen generation, is deactivated the by sulphur deprivation (Melis et al. 2000). They demonstrated H_2 production in a sulphur-depleted, sealed, illuminated *C. reinhardtii* culture for several days, starting one day after sulphur deprivation (Melis et al. 2000). In a first step the algae was grown in a medium containing acetate until a high biomass concentration was obtained. Upon harvesting, the biomass slurry was transferred to a sulfur-deprived medium in a second step. Sulphur deprivation causes a progressive decrease in the photosynthetic O_2-evolving capacity of the cells, because the PSII repair function is slowed nearly to a halt (Wykoff et al. 1998; Melis et al. 2000). When the photosynthesis rate drops below the level of respiration, the culture becomes anaerobic in a short period time as long as no oxygen is present in the photobioreactor (Melis et al. 2000). Under these conditions *C. reinhardtii* is able to synthesize an [Fe-Fe]-hydrogenase which combines electrons and protons from a remaining PSII activity and especially from the degradation of the starch (that has been accumulated in first stage 1 of the whole process) to produce significant amounts of H_2 for several days (Antal et al. 2003; Posewitz et al. 2004; Rupprecht et al. 2006; Hemshemeier et al. 2008; Chochois et al. 2009). In all the green microalgal species analyzed so far hydrogenases are coupled to the photosynthetic electron transport chain via ferredoxin, which after being reduced by PS1 donates its electrons to the hydrogenase, as has been shown for *C. reinhardtii* (Winkler et al. 2009).

This chapter addresses the main aspects to be tackled in the design of photobioreactors for the photobiological production of H_2 from green microalgae when using the route proposed by Melis and co-workers. For economic reasons, the growth phase should be performed first in raceways open ponds. Those systems are not appropriate for the H_2 production phase since the collection of the

desorbing hydrogen would pose serious difficulties unless fully sealed closed photobioreactors were used. Figure 13.1 schematically illustrates a typical process flow envisioned for continuous photobiological hydrogen production at industrial scale.

The photobioreactor configuration proposed in Fig. 13.1 could also be used, with slight operational modifications and the establishing the proper physiological conditions, for the production of H_2 by indirect biophotolysis with cyanobacteria. Thus, in case the selected strain for producing H_2 is a cyanobacteria, the biomass production step could be carried out in the open photobioreactor and the subsequent H_2 evolving step in the closed tubular system (Fig. 13.1a). To that end, if tubular technology were used in the H_2 production step not even a O_2-free airstream can be used for degassing as both enzymes [Ni-Fe] hydrogenase and nitrogenase (depending on the cyanobacteria used) are inhibited by any nitrogen source. Any N_2 could be assimilated through the heterocysts of the cyanobacteria. Therefore, when using the tubular technology with cyanobacteria in this step, the centrifugal pump employed to drive the culture through the circuit would also have to be used to transport, coalesce and separate the H_2 bubbles that would gather in the upper part of the tubes and collect them in the degasser. H_2 removal in these conditions can be further favoured by a partial vacuum established to this purpose in the headspace of the degasser. On the other hand, the schemes proposed in Fig. 13.1a, b, could be used for producing H_2 by a photo-fermentative process of the biomass produced in the open raceway by using PNS bacteria to degrade the organic material (i.e., biomass coming from the open raceway) in the enclosed photobioreactors. Therefore, according with the photosynthetic microorganism used, the scheme of Fig. 13.1 might be used for producing H_2 by means of both photolytic and photofermentative routes. The number of modules required will depend on the biomass productivity of the first step. Details about how estimate them depending on the microorganism and technology used in this second step are described later (see scale up section for each type of technology). Finally, the depleted biomass can be used as a feedstock for biofuel. Depending on the downstream process chosen for this biomass (thermochemical, anaerobic digestion, direct transesterification, etc.) the characteristics of the produced biofuel will be different (bio-oil, biogas, biodiesel, etc.).

Regardless the photobioreactor used in either the first step of biomass production or in the hydrogen production phase, the photobioreactor must be designed and operated to meet the optimal conditions required for the microalgal strain in each phase of the process, making clear how important is to know what the main factor determining growth rate either phase are.

III. Major Factors Impacting on Photobioreactor Performance

Microalgae, like all living microorganisms, require the proper conditions to grow. The best the culture conditions the higher the growth rate and productivity obtained. Thus, the pH, temperature and culture medium must be those appropriate for the microalgae. The mineral culture medium can be easily supplied so as to not limit the growth; however, the correct supply of light requires a deep analysis due to its different nature with respect to mineral nutrients. In the same way, CO_2 must be supplied to meet the carbon demand and maintain the proper pH in the culture. At the same time, the assimilation of CO_2 provokes the consumption of water and the generation of oxygen that must be removed. This consequently impacts the required mass transfer capacity of the culture system. In addition, the power supply to maintain the cells in suspension and reduce light and nutrient gradients within the culture must be considered, keeping in mind that inadequate fluid dynamics can have deleterious effects on fragile microalgal cells. Finally the control of temperature is mandatory to ensure the optimal temperature to grow and also to prevent overheating.

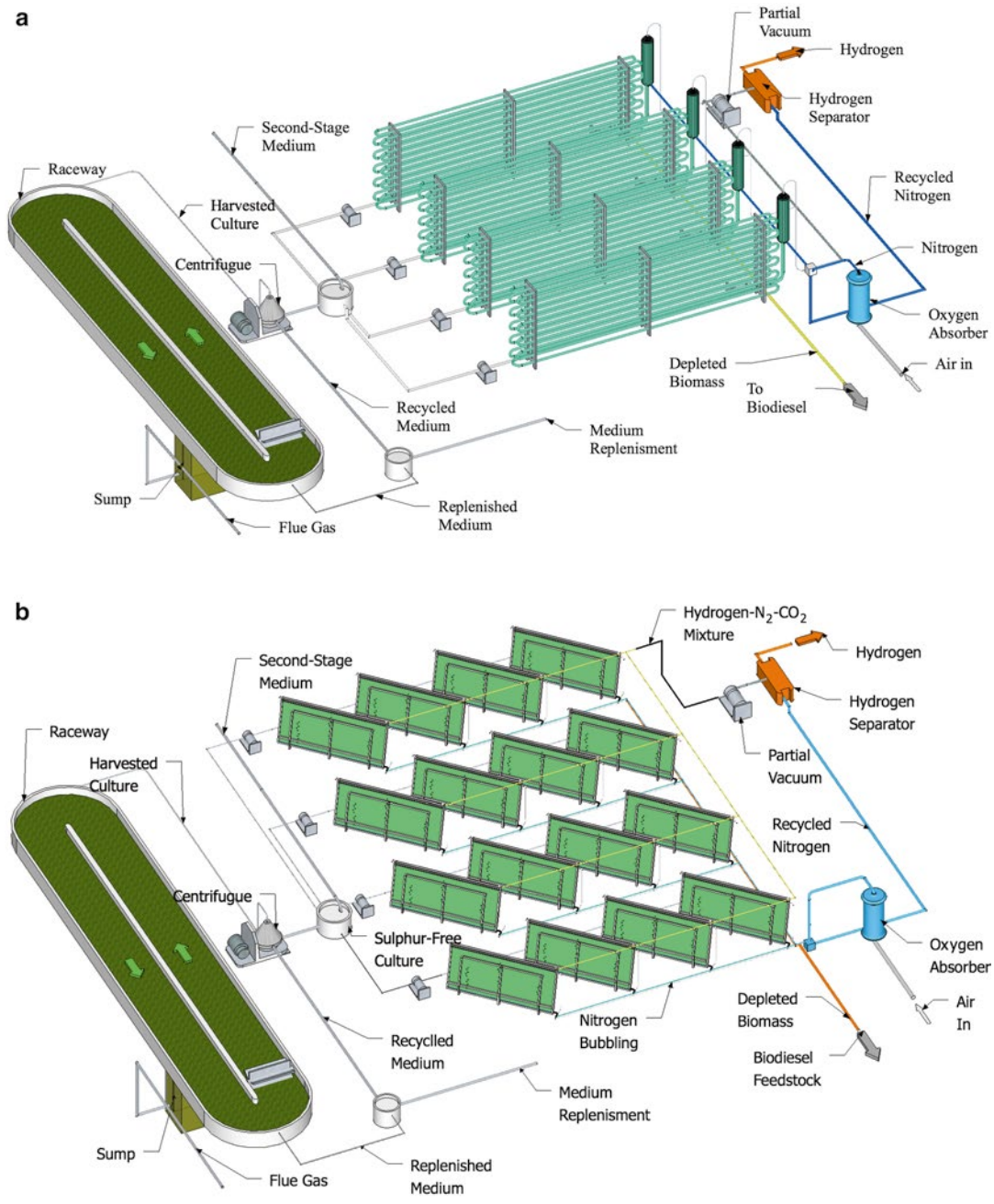

Fig. 13.1. Conceptual scheme of an integrated, microalgae-based, continuous two-step process for H_2 production with tubular PBR (**a**) or flat plate reactor (**b**). The biomass from the raceway reactor of the first step is harvested by centrifugation. The daily harvested slurry is then transferred to the appropriate culture medium and drove to the closed reactors by centrifugal pumps. The H_2 produced is stripped by bubbling in the degasser an *in situ* prepared O_2-free airflow (bubble column or the entire culture, for tubular PBR or flat plate reactor, respectively). Upon separated the H_2 from the rest of gases, mainly N_2 and a small amount of CO_2, the O_2-free gas is recycled. Finally the depleted biomass can be used for additional biofuels. The most appropriate technology to use in the H_2 production step (flat plate or tubular) and culture medium are depending of the microorganism used for producing H_2. For details about the selection of technology, culture media, procedures for producing the O_2-free airflow and downstream processing possibilities for the depleted biomass (see text).

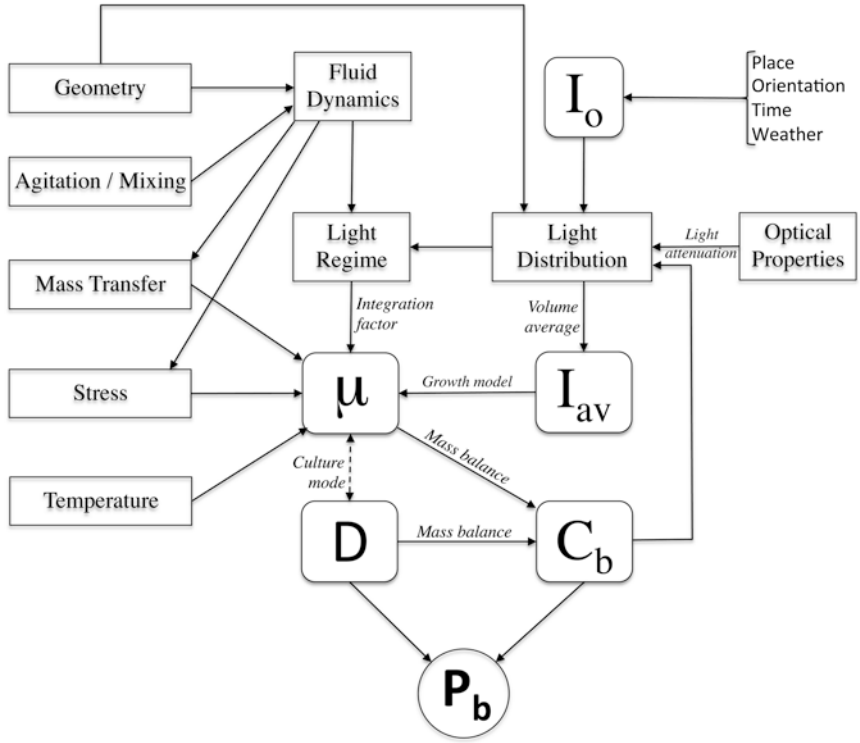

Fig. 13.2. Relationships between the major factors influencing biomass productivity of microalgal mass cultures. Incident irradiance (I_o) promotes microalgal growth. The biomass productivity (P_b) is the result of multiplying biomass concentration (C_b) by the specific growth rate (μ), which is a function of light availability (calculated as average irradiance I_{av}). In continuous cultures, the dilution rate (D) equals μ in steady state (Adapted from Molina 1999 and Molina et al. 2010).

Figure 13.2 shows the main factors impacting on biomass productivity and their relationships, whatever the outdoor photobioreactor used (open or closed). Light availability inside the photobioreactor and temperature have been found to be the main factors determining optimum system performances (Molina Grima 1999). Thus, when the temperature of the culture is kept within an appropriate interval, light availability is the only factor limiting growth. The productivity is determined by the growth rate (μ) and the biomass concentration (C_b), which is a function of the light distribution inside the photobioreactor and the light regime at which the cells are subjected. Once this function is known, it is possible to obtain a correlation between biomass productivity and the average irradiance within the reactor (Acién-Fernández et al. 1998). On the other hand, average irradiance within the reactor is a function of the irradiance impinging on the reactor surface (I_o), which comes as a consequence of the geographic and environmental factors (Acién-Fernández et al. 1997, 2012). The geographic location and day of the year determine the solar incident radiation and therefore the temperature in the culture. While temperature can be kept within a narrow interval by using suitable thermostatic systems, solar radiation cannot be controlled.

The incident solar radiation, which is a function of climatic and geographic parameters of the facility location (Incropera and Thomas 1978), as well as the design and orientation of the photobioreactor (Lee and Low 1992; Qiang and Richmond 1996; Sierra et al. 2008), determines the maximum energy available for growth. The incident solar radiation is attenuated inside the photobioreactor in a way that depends on the geometry, the biomass concentration and the optical properties of the biomass. Thus, a heterogeneous light distribution always takes place inside

dense microalgal cultures (Molina Grima et al. 1994; Acién-Fernández et al. 1997). The light availability or average irradiance inside the culture can be calculated by a volumetric integration of the irradiance profile. The cell metabolism adapts to this light availability and so does the biochemical composition and growth rate (Acién-Fernández et al. 1998). On the other hand, the photobioreactor fluid dynamics also determine the mass transfer and the light regime of the cells. The latter is the result of the distribution of residence times between light and dark zones (Phillips and Myers 1954; Terry 1986; Grobbelaar 1994). This light regime affects the photosynthetic efficiency of the cultures, modulating the use of the available light calculated as averaged irradiance (I_{av}). High mixing favours an adequate light regime and thus an efficient use of light although the mixing power supplied to the cultures must not reach intensities that can damage the individual cells by hydrodynamic stress.

The biomass concentration is influenced by the growth rate. Biomass accumulation is the result of a mass balance between biomass generation (μ) and the output rate that can be expressed as a dilution rate (D) in continuous or semicontinuous cultures. Both, growth rate and biomass concentration, determine the final biomass productivity of the system. Thus, in an optimum system where there are no limitations other than light, a direct interrelationship between light availability, rate of photosynthesis and productivity may be expected. In fact, it seems that other limitations do not only limit growth through their direct effect, but also impose a limitation on the ability to utilize the absorbed solar energy. Therefore, in the end the most important design criterion will be to enhance the light availability per cell and consequently high efficiency in transforming the sunlight reaching the culture.

IV. Principles for Photobioreactors Design and Scale Up

According with the envisioned scheme of Fig. 13.1, for the hydrogen production step, a PBR with high surface to volume ratio is mandatory to obtain high cell densities, maximum interception of light per unit of occupied area, a good light distribution within the reactor and an efficient H_2 removal to overcome product inhibition (Akkerman et al. 2002; Posten 2009). Flat plate reactors (FPRs), alveolar plate reactors and tubular reactors may provide such a high surface to volume ratios. These culture systems may provide the requested mass transfer capabilities for stripping the dissolved H_2 from the culture and maintain the temperature of the culture within acceptable limits. This section describes the basic principles for designing both the open raceway (RWs), to be used for the preparation of the inocula, and closed reactors needed in the scale up of a process for photobiological production of hydrogen with microalgae.

A. Open Raceway (RW) Reactor

The principles for the design and construction of shallow paddle-stirred raceways for large microalgal production (Oswald and Golueke 1968) were reviewed by Oswald (1988) and recently have been updated by Chisti (2013) and Acién-Fernández et al. (2013). A theoretical approach to modelling microalgae growth in raceway reactors, taking into account the biological and hydrodynamic phenomena occurring in the reactor, has recently been reported (James and Boriah 2010). A photograph of an open 100 m^2 set-up at the authors' facility is showing in Fig. 13.3.

Selection of a suitable bottom lining and wall construction are important to the success of the open pond. The lining may be made of concrete, sheets of plastic or rubber material. The stirring is accomplished with one paddle wheel per pond to match the designed liquid depth for the raceway. The presence of deflectors in the bends also improves the performance of the RW by enhancing the liquid velocity and reducing the power consumption for the same liquid velocity. Recently the use of asymmetric islands to minimize existence of dead zones in the bend areas and maximize the energy yield has also been reported (Chisti 2013). A wheel of large diameter (ca. 2.0 m in

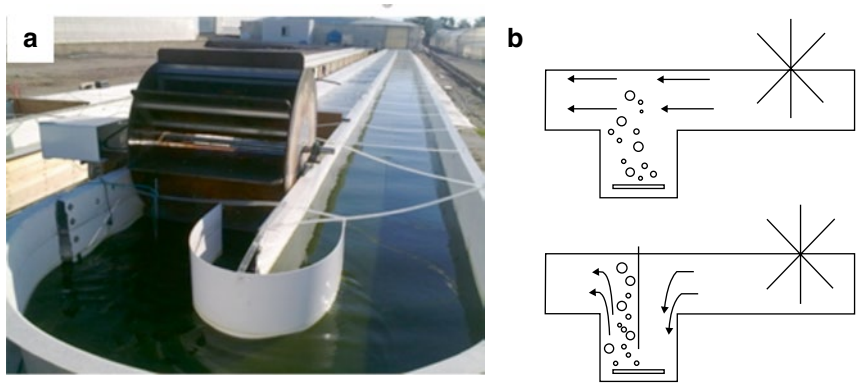

Fig. 13.3. Image of an open 100 m^2 raceway set-up at the authors' facilities (**a**), and scheme of the sump configurations tested (**b**). The channel length is the distance travelled by the culture from the discharge side of the paddle wheel to the entering side.

diameter) revolving slowly (e.g. 10 rpm) is preferable to smaller diameter wheels that have to rotate faster and produce excessive shear damage and foam. Under these conditions biomass concentrations of up to 1.0 $g \cdot L^{-1}$ and productivities of 0.1 $g \cdot L^{-1} \cdot d^{-1}$ are possible. The two major technical issues to keep in mind at the time of designing an open RW are related to the poor gas-liquid mass transfer and mixing capability of the current industrial scale reactors which have a great impact in RW performance.

1. Mass Transfer. The Supply of Carbon Dioxide and the Removal of Oxygen in an Open RW

Several systems have been developed to supply CO_2 efficiently to shallow suspensions. In most cases the gas is supplied in form of fine bubbles. Due to the shallowness of the suspension the residence time of the bubbles is not sufficient for the CO_2 to dissolve and a significant part of the CO_2 supplied is lost to the atmosphere. For this reason, raceway reactors are frequently equipped with devices such as sumps or mixing columns to increase the gas/liquid contact time (Azov and Shelef 1982; Weissman and Goebel 1987; Weissman et al. 1988; Doucha et al. 2005; Moheimani and Borowitzka 2007; Park and Craggs 2010; Park et al. 2011; Putt et al. 2011). An arrangement frequently used to attain this is to install a baffle dividing vertically the sump in two sections of ascending and descending liquid (Fig. 13.3b). In this sump configuration the culture velocity in the descending section can be adjusted to match the ascension of the small CO_2 bubbles. Using this technique, Laws et al. (1986) reported a 70 % efficiency in CO_2 transfer, a large improvement compared with the 13–20 % efficiency obtained when gas is injected in the shallow channel. The use of sumps is the simplest way to improve carbonation in raceways because they can be easily incorporated in the channels and do not need an external energy supply. However, we have carried out experiments with and without baffle with the raceway pond shown in Fig. 13.3a, and the usefulness of introducing a baffle into the sump is questionable. There was a slight increase of the mass transfer capacity in the sump in the experiment at the expense of increased power consumption and a reduction in the culture velocity and the mixing degree in the system. In the authors' opinion the sump configuration with baffle for the counter-current injection of CO_2 should be considered as a serious disadvantage. The CO_2 transfer under both sump configurations was tested in the same experimental set up and similar CO_2 uptake efficiencies in the sump were achieved (>95 %).

On the other hand, oxygen desorption has been usually disregarded in the design of these type of photobioreactors. Thus, oxygen removal is performed through the culture surface the mass transfer coefficient being extremely low and oxygen accumulating into the culture (Jiménez et al. 2003). It has

been previously reported that, in large ponds with small water circulation and turbulence, O_2 concentration may reach concentrations as high as 500 % saturation, inhibiting photosynthesis and growth, and eventually leading to culture death (Vonshak 1997).

The mass transfer capacity of the system (i.e., *Kla* coefficient) and mixing (given by both mixing time and dispersion coefficient) are key parameters to be considered in the proper design of a raceway system for CO_2 supplying and for removal of the photosynthetic oxygen generated. As the oxygen generation rate is about 1.3–1.4 g O_2 per gram of biomass and that the CO_2 consumption rate is roughly 2 g per gram of biomass produced, the minimum *Kla* values which would be requested for satisfying an appropriate mass transfer capacity in a raceway are much higher (one order of magnitude greater) than those currently provided in the existing industrial raceway reactors. Taking into account that, it makes no sense to supply CO_2 in the channel because in this zone the mass transfer capacity is virtually zero, the only zone available for CO_2 supplying is the sump. On the other hand, for O_2 degassing the available zones are the sump and the zone of the paddle wheel. Nonetheless, the only practical way to increase the O_2 removal, for a determined paddle wheel configuration rotating at a specific frequency, is by increasing the relative volume of the sump with respect the total volume of the raceway and by increasing the depth of the sump.

2. Mixing and Power Consumption

The evolution of the open culture technology is the consequence of the development of the mixing systems that have been designed in the time. Mixing is necessary in order to prevent the cells from settling and sticking to the bottom and to avoid thermal stratification of the culture. Mixing is of paramount importance since it is directly linked to other key parameters (Fig. 13.2). Mixing determines the light-dark cycling frequency, improves the mass transfer capability of the culture system, reduces the mutual shading between cells and decreases the potential photoinhibition effect at the pond surface. Properly designed paddle wheels are by far the most efficient and durable pond mixers. They discharge all of the culture entering the system and are thus highly efficient. With reference to Fig. 13.3a, the design is based in a culture flowing at depth d in a channel with finite width, w, and unspecified length, L. Water depth (d) is maximum just after the discharge side of paddlewheel and minimum in the entering side. This depth reduction (Δd), termed head loss or depth change, determines the rate of energy that must be provided to maintain circulation at the chosen velocity. The head losses (energy dissipation) depend on: (i) flow around the two 180° curves (bend losses) and (ii) the friction with the surface (side wall and bottom). The head losses as water flows in bends is calculated by (Acién-Fernández et al. 2013):

$$\Delta d_b = \frac{k \bullet v^2}{2g} \tag{13.1}$$

where v is the mean velocity (ms^{-1}); g the acceleration of gravity (9.8 ms^{-2}) and k is the kinetic loss coefficient for each bend. Similarly, the channel and wall friction loss, Δd_c, can be calculated by (Acién-Fernández et al. 2013):

$$\Delta d_c = v^2 n^2 \frac{L}{R^{4/3}} \tag{13.2}$$

where n is the roughness factor; R (m) is the channel hydraulic radius: $R = 4w \cdot d/(w+2d)$ and L the length of the channel (m). The total head loss or change in depth is $\Delta d = \Delta d_b + \Delta d_c$. The channel length, L, that corresponds to the calculated head losses for a given friction factor and a culture velocity (v) is given as Eq. (13.3):

$$L = \frac{\Delta d \left(dw / \left(w + 2d \right) \right)^{4/3}}{v^2 \bullet n^2} \tag{13.3}$$

where n is the Manning friction factor ($s \cdot m^{-1/3}$), L is the channel length that corresponds to the head loss (Δd) and w is the channel width. The value of n varies according

to the relative roughness of the channel. Experimentally determined n values in algae growth channels vary from 0.008 to 0.030, the former for smooth plastic-lined channels and the latter for relatively rough earth. The channel velocity, v, impacts on the paddle wheel's power requirements, calculated as:

$$P = \frac{Q \cdot \rho \cdot g \cdot \Delta d}{\eta} \tag{13.4}$$

where P is the power (kW); Q the culture flow rate in motion ($m^3\ s^{-1}$); ρ is the specific weight of culture ($kg \cdot m^{-3}$); g is the gravitational acceleration ($m\ s^{-2}$); Δd is the change in depth generated in the paddle wheel (m) and η is the efficiency of the paddle wheel, which usually is about 0.2. Because Δd is a function of v^2, the power consumption, P, increases as the cube of velocity. It is therefore worthwhile to minimize velocity whenever energy is a major cost factor. Typical values of flow rates range between 15 and 30 $cm \cdot s^{-1}$, whereas the power supply is around 2–4 $W \cdot m^{-3}$. Velocities greater than 30 $cm \cdot s^{-1}$ will result in large values of Δd in long channels and may require high channel walls and higher divider walls.

The mixing time reduces when liquid velocity through the system increases and the channel length-to-width ratio (L/w) decreases. For the system shown in Fig. 13.3a this L/w ratio is about 100 and the mixing time is about 2 h, when no baffle is inserted, or about 5 h when the baffle is inserted in the sump (Acién-Fernández et al. 2013). A more accurate quantification of mixing in the different zones of the raceway can be achieve by measuring the Bodenstein number (Bo) which is related to the dispersion coefficient (Dz) by (Verlaan et al. 1989):

$$Dz = \frac{v L_{section}}{Bo} \tag{13.5}$$

where $L_{section}$ represents the length of each zone within the reactor (channel, sump, paddlewheel and bends). As a rule of thumb, when Bo is ≤ 20 (i.e., high dispersion coefficient) the mixing pattern in that raceway zone is a perfect mixing and when Bo is ≥ 100 the pattern corresponds to a plug flow. Overall, in an industrial raceway pond with a length to width ratio over 50, the sump, paddle wheel and bends shows a complete mix pattern and in the channel however the pattern corresponds to a completely plug flow.

3. Scale-Up of Raceway Reactors

Reactor scale-up is based on reactor surface area rather than volume. An open RW facility capable of providing the necessary biomass for the H_2 production step (closed PBR described in Fig. 13.1) will require the RW facility running in continuous or semicontinuous mode (the biomass productivity in continuous mode is at least 2.3 times greater than in batch mode, and generally about five times greater). The question to solve in the scale up is to calculate the land demand of a RW facility and the number of raceway units needed for producing M tonnes of biomass (dry weight) per year of a specific microalgae. The tools for designing this facility are described next.

The growth rate of the strain can be calculated by Eq. (13.6) (Molina Grima et al. 1994).

$$\mu = \frac{\mu_{max} I_{av}^{\ n}}{I_k^n + I_{av}^{\ n}} \tag{13.6}$$

In Eq. (13.6), the maximum specific growth rate, μ_{max}, the light saturation constant, I_k, and the shape parameter, n, are kinetic parameters which are species specific and must be determined experimentally. In Eq. (13.6), I_{av} represents the average irradiance within the raceway that can be estimated by:

$$I_{av} = \frac{I_o}{K_a \cdot d \cdot C_b}\left(1 - \exp\left(K_a \cdot d \cdot C_b\right)\right) \tag{13.7}$$

Equation (13.7) is a simplified model to calculate I_{av}. This model is suitable for any combination of disperse and direct light as long as it is impinging uniformly on the reactor surface (Molina Grima et al. 1996; Acién-Fernández et al. 1997). According to

this model, the average irradiance, I_a, is a function of the irradiance measured on the reactor surface, I_o, the extinction coefficient of the biomass, K_a, the optical light path (depth of the culture), d, and the biomass concentration in the culture, C_b.

The average volumetric biomass productivity (g L^{-1} d^{-1}) all year long in a continuous, or semicontinuous, culture is determined by:

$$P_{bv} = D \cdot C_b \tag{13.8}$$

where D is the average dilution rate all through the year (d^{-1}) and C_b the average biomass concentration during the year (g L^{-1}). As a rule of thumb, D is about 40 % the maximum specific growth rate of the strain and ranges between 0.2 and 0.5 d^{-1} for winter and summer time, respectively (Acién-Fernández et al. 2013). From Eq. (13.8), it is possible to calculate the areal productivity P_{ba}, taking into account the volume to surface ratio of the culture system.

$$P_{ba} = P_{bv} \frac{V}{S} \tag{13.9}$$

The V/S ratio is a function strongly dependent on the culture depth, d, and ranges between 150 and 250 L m^{-2} for depths of the culture in the raceway fluctuating between 15 and 25 cm, respectively. On the other hand, the land demand S (m^2) i.e., the mixable area of raceway, for producing the M tonnes of biomass a year is related to P_{ba} by means of:

$$S = 2.74.10^3 \frac{M}{P_{ba}} \tag{13.10}$$

Note that, for a finite value of the channel width, w, the permissible mixing channel length, L, and thus the mixable area, $S = L\,w$, is a function strongly dependent on depth, d. From Eq. (13.10), we can determine the number of raceway units needed, taking into account that the optimal mixable surface of raceway should not exceed 0.5 ha and that, as a rule, the typical permissible length (Eq. 13.3) to raceway width ratio (L/w) is about 30–50.

B. Closed Photobioreactors

A completely sealed photobioreactor is needed in the H_2 production phase. The two technologies already tested at lab scale, which may be useful in this step are the flat panel and the tubular systems. These reactors meet a set of conditions: (1) low optical path, i.e., a high surface to volume ratio (S/V), so that the average irradiance within the culture is high; (2) high biomass concentrations (around 1 g L^{-1}), which may provide a chlorophyll content of about 20–30 mg chl *a* L^{-1}, which facilitates the use of the maximum number of photons (direct and diffuse light) impinging on the reactor surface; and (3) these reactors can be easily implemented with a proper degassing system in order to remove all the produced H_2 and, at the same time, to maintain the appropriate fluid-dynamic conditions to enhance the mass transfer and light distribution within the reactor.

In both photobioreactors the H_2 produced can be stripped out of the reactor by maintain a partial vacuum (roughly −4 kPa) (Giannelli et al. 2009) in the headspace (upper part) of the flat panel or the headspace of the degasser (bubble column) in the tubular photobioreactor, respectively. In these conditions, the culture is oversaturated and close to cause bubbles of pure H_2 forming in the culture. However, the H_2 can be kept under saturating concentrations by stripping it with O_2–free-air flow bubbled through the reactor in the case of flat panel, which also provides mixing and allows working at the proper fluid dynamics conditions within the culture; or through the bubble column (degasser system) in the case of the tubular technology. This O_2-free gas can be obtained by bubbling air through a sulphite solution before entering to the PBR. The sodium sulphite is oxidized to sodium sulphate by the O_2. The concentration of sodium sulphite in the absorber should never be below 0.5 M. This guarantees a O_2-free airflow in the gas leaving the O_2 absorption column (Camacho Rubio et al. 1991, 1999), that can be used for removal the H_2 produced in the closed photobioreactor.

Table 13.1. Mass transfer coefficient required for the stripping out of the H_2 produced as a function of hydrogen production rates (r_{H2}) reported.

Microorganism	PBR type	Reported H_2 production rate	Calculated production rate (r_{H2}) ($molH_2/L \cdot h$)	Kla (1/h)	References
Green alga *C. reinhardtii*	Tubular 110 L	0.62 ml/L·h	2.77E-05	0.90	Giannelli and Torzillo (2012)
Green alga *C. reinhardtii*	Benchtop n.a.	200 mmol/gchla·h	2.00E-03	2.35	Winkler et al. (2002)
Green alga *C. reinhardtii*	Benchtop n.a.	13 ml/L·h	5.80E-04	0.68	Laurinavichene et al. (2006)
Green alga *S. obliquus*	Benchtop n.a.	150 mmol/gchla·h	1.50E-03	1.76	Florin et al. (2001)
Cyanobacterium *A. variabilis*	Benchtop helical reactor ~ 2 L	167.6 mmol/gchla·h	1.68E-03	1.97	Sveshnikov et al. (1997)
Cyanobacterium *A. variabilis*	Benchtop flat plate, 2 cm	4.1 L/kg·h	1.83E-04	0.22	Yoon et al. (2006)
Cyanobacterium *A. variabilis*	Benchtop flat plate, 4 cm width	0.45 L/kg·h	2.01E-05	0.02	Yoon et al. (2006)
Cyanobacterium *A. variabilis*	Benchtop Flat plate, 2 cm width	5.6 L/kg·h	2.50E-04	0.29	Berberoglu et al. (2008)
PNS bacterium *Rp. palustris*	Tubular 50 L	27.2 ml/L·h	1.21E-03	35.72	Adessi et al. (2012)
PNS bacterium *Rb. spharoides*	Benchtop Flat plate	5.9 mol/kg·h	5.90E-03	6.94	Sasikala et al. (1991)

Mass transfer capacity required has been calculated considering that O_2-free air is bubbled into the culture to remove hydrogen ($[H_2^*] = 1.06 \cdot 10^{-7}$ mol/L) and that the culture become saturated with pure hydrogen ($[H_2]_{sat} = 8.50 \cdot 10^{-4}$ mol/L)

The hydrogen desorption capacity, N_{H2}, is calculated as a function of the volume of the mass transfer unit, V_{mt}, (i.e., the entire culture volume in the case of flat panel, or the culture volume contained inside the degassing bubble column in the case of tubular reactors), the volumetric mass transfer coefficient, $K_l a_{l,H2}$, and the driving force for hydrogen desorption. The latter is calculated as the difference between dissolved hydrogen in the culture, $[H_2]$ and the dissolved hydrogen in equilibrium with the gas phase which is in contact with the liquid, $[H_2^*]$, i.e., oxygen-free air (Eq. 13.11). The dissolved hydrogen concentration in equilibrium with gas phase is calculated according to Henry's law for diluted gases under ideal conditions, as a function of Henry's constant H_{H2}; total pressure, P_T, and the molar fraction of hydrogen in the gas phase, y_{H2} (Eq. 13.12).

$$N_{H2} = K_l a_{l,H2} \left([H_2] - H_2^* \right) V_{mt,H2} \tag{13.11}$$

$$H_2^* = H_{H2} P_T y_{H2} \tag{13.12}$$

The molar fraction of H_2 in air is $1.0 \cdot 10^{-4}$, then the hydrogen molar fraction in O_2-free air, y_{H2}, is $1.25 \cdot 10^{-4}$, whereas the molar fraction of hydrogen in pure hydrogen gas is 1.00. Considering that the Henry's law constant for H_{H2} is 8.50 10^{-4} mol $L^{-1} \cdot atm^{-1}$, at 25 °C, it is possible to determine the required value of the mass transfer coefficient to strip the dissolved H_2 accumulated in the culture as a function of hydrogen productivity and hydrogen concentrations in the liquid and gas phase (Eq. 13.11). Table 13.1 shows the calculated $K_l a_l$ values needed for the desorption of H_2 by using an O_2-free airflow ($y_{H2} - 1.25 \cdot 10^{-4}$), for selected H_2 production

rates, r_{H2}, reported, considering that the liquid become saturated in equilibrium with pure hydrogen. These values are easy to achieve in flat panels, and feasible with more difficulty in tubular reactors

$$K_l a_{l,H2} = \frac{P_{H2} V}{\left([H_2] - [H_2^*] \right) V_{mt,H2}} \qquad (13.13)$$

1. Flat Panels

Flat panels are transparent plates joined close together so that they contain the culture, Thus, they can be illuminated by one or both sides and stirred by bubbling the O_2-free airflow. The dimensions of flat panels are variable but a height under 1.5 m and a separation between plates shorter than 0.10 m are preferred, to avoid the use of high mechanical resistance materials (Fig. 13.4).

Pulz and Scheibenbogen (1998) used flat panels with inner walls arranged to promote an ordered horizontal culture flow that was forced by a mechanical pump (Fig. 13.4). The most innovative aspect of the commercially available Pulz's reactor was that several parallel plates were packed together; close enough to attain up to 6 m^3 of culture volume on 100 m^2 of land, which at the same time improves the dilution of light, with a total illuminated culture surface of ca. 500 m^2. This flat alveolar reactor has no gas headspace and the entire volume of the panel is filled with the culture. The research of Hu et al. (1996) resulted in a type of flat plate reactor made of glass sheets, glued together with silicon rubber to make flat vessels. This simple methodology for the construction of glass reactors provided the opportunity to easily build up reactors with any desired light-path. Doucha et al. (1996) described an optimized large-scale flat plate photobioreactor module of 1,000 m^2. Recently, a new design of vertical flat panel photobioreactor consisting of a plastic bag located between two iron frames has been proposed (Rodolfi et al. 2009); this brings a substantial cost reduction to this type of reactors but the system is not completely sealed as it is required for H_2 production. The O_2-free aeration is done through a PVC plastic tube perforated to provide minute holes of about 1 mm. A separate degasser must be used in the case of the alveolar flat plate reactor. The cooling system is a heat exchanger inserted in the reactor. The mass transfer, mixing and heat transport capacities in flat panel reactors are usually very good. The main advantages of this reactor type are the low power consumption (roughly 50 W m^{-3}) and the high mass transfer capacity (Kl_la_l=25 h^{-1}). The major technical issues in designing and building up this type of reactors are (1) the panel orientation and light path depth, (2) the O_2-free aeration rate for both maintaining the proper fluid-dynamic and removal of H_2, and its impact on power supply, mass transfer and mixing; and (3) the temperature control.

a. Panel Orientation and Light Path Depth

The solar radiation intercepted may vary significantly with orientation and position. For latitudes above 35°N the east-faced/west-faced orientation are favourable to north/south, the higher the latitude the higher the increase in the solar radiation intercepted. On the contrary, for latitudes under 35°N the north/south-orientated reactors intercept more radiation and the difference is more pronounced the closer to the equator (Acién-Fernández et al. 2013). The position of the reactor also influenced the type of radiation intercepted. In vertical panel PBR the proportion of disperse radiation is dominant (Qiang et al. 1996; García Camacho et al. 1999). Vertically arranged flat panels intercept less solar radiation than inclined flat panels but have the advantage of less cost and overheating. The vertical arrangement allows reducing solar radiation peaks at noon increasing the interception of solar radiation in the morning and afternoon. Moreover, the vertical arrangement also shows an improved interception of solar radiation in winter with respect to summer (Sierra et al. 2008). Disperse radiation has been consistently

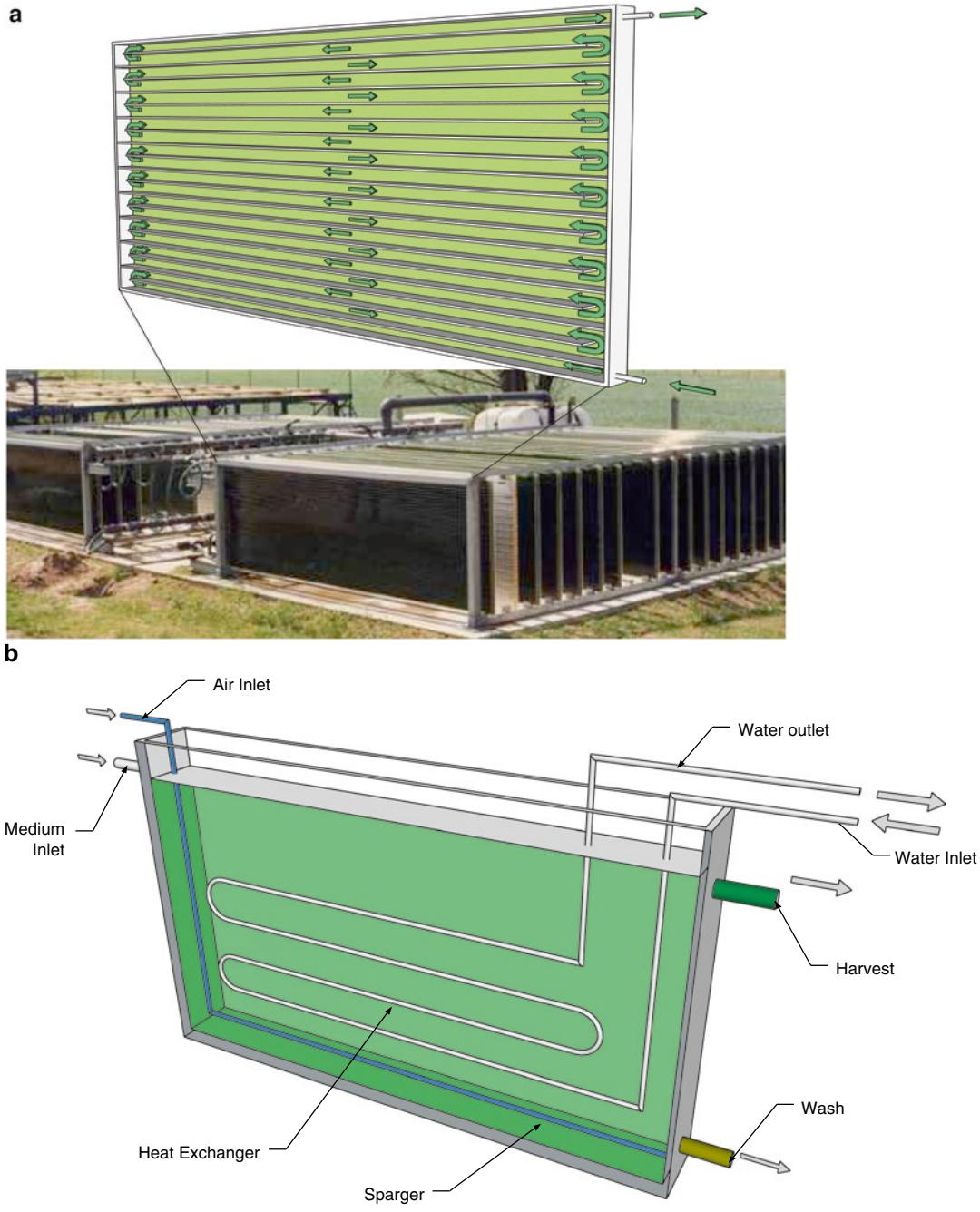

Fig. 13.4. Image of an alveolar flat plate photobioreactor field (**a**) (Courtesy of Dr. O. Pulz, IGV GmbH, Nuthetal, Germany). Detail shows the horizontal channels through which the culture is circulated. Below. (**b**) Is a scheme of a non-alveolar flat plate reactor in which the appropriate fluid-dynamic conditions are provided by bubbling O_2-free airflow at the bottom contributing, at the same time, to strip out the dissolved hydrogen produced.

reported to be more efficient for microalgal cultures. Indeed, the photosynthetic efficiency of vertical photobioreactors has resulted higher than optimal-tilt reactors, reaching values of 20 % (Qiang et al. 1996). This is due to the fact that low irradiance levels normally result in higher photosynthetic efficiencies; this is, when cells are growing under irradiance levels far from saturating light assimilation is more efficient. This can be accomplished by increasing the light-receiving surface of photobioreactor per square meter of occupied land, a technique usually referred to as "dilution" of light.

With respect to the panel depth, to maintain average irradiances over 100 $\mu E \cdot m^{-2} \cdot s^{-1}$ in flat panels while maintaining a cell density about 1 g L^{-1} the panel depth should be below 7 cm (typically 4–6 cm) in order to achieve chlorophyll concentrations in the range of 20–30 mg chl *a* L^{-1} for an increased light-to-H2 conversion efficiency.

b. O_2-Free Aeration Rate and Its Impact on Power Supply, Mass Transfer and Mixing

The power input per volume unit due to aeration, P_G/V_L, in a flat panel reactor is a function of aeration rate, the density of the liquid, ρ_L and the gravitational acceleration, g and can be calculated:

$$\frac{P_G}{V_L} = \rho_L g U_G \tag{13.14}$$

where U_G is the superficial gas velocity in the O_2-free aerated zone. U_G is easily derived from the O_2-free airflow rate, in v/v/m, multiplying this by the total volume of the culture and dividing by the cross-sectional area of the aerated zone. The power supply also impacts on the mass transfer capacity of the flat panel reactor according to the following equation:

$$K_L a_L = 2.39 \cdot 10^{-4} \left(\frac{P_G}{V_L} \right)^{0.86} \tag{13.15}$$

Note that, in spite of the low power supply used, the volumetric mass transfer coefficient $K_l a_l$ reached values of about 25 h^{-1}, enough to avoid dissolved hydrogen accumulation with O_2-free air (Table 13.1). This mass transfer capacity in the flat panel photobioreactor can be attained with a power supply of 50 W m^{-3}. The low power supply requirement and the relatively high mass transfer capacity are important advantages of the flat panel photobioreactor because of the sensitivity to stress caused by intense turbulence that show many microalgal strains. In addition to mass transfer capacity, the power supply also determines the mixing time inside the rector. In the range of typical aeration rates: 0.05–0.35 v/v/min (i.e., power supply between 5 and 55 W m^{-3}) the complete mixing in the flat panel photobioreactor ranged between 150 and 100 s, much lower than those obtained in tubular systems and open raceway.

In the case of alveolar panel reactor, the culture is forced to circulate through the internal channels by means of a centrifugal pump. In these systems, thus, there is no headspace in the reactor body and the supply of O_2-free gas has to be carried out in an auxiliary degasser connected to the reactor body, in a similar implementation as in tubular technology. Therefore the assessment of the power consumption, mass transfer and mixing is analogous to tubular technology.

c. Temperature Control

Flat panels can be cooled by water spray or alternatively by using internal heat exchangers. According to the authors' experience, the cooling capacity of spray systems is limited and its application is only possible under certain environmental conditions (temperature, humidity, etc.). Most times the use of a heat exchanger is needed. The reduction of solar radiation interception in the vertical arrangement also allows reducing the overheating of the cultures at noon, thus reducing the requirements of cooling. In any case, the heat transport capacities in flat panel reactors are usually very good. The values of the heat transfer coefficient in these systems range from 300 to 1,000 $W \cdot m^{-2} \cdot K$ (Sierra et al. 2008).

The design of the tubular heat exchanger can be done from the following heat balance:

$$m_{water} \cdot Cp_{water} \cdot \left(T_{outlet} - T_{inlet}\right) = U \cdot A \cdot \frac{\left(T_{culture} - T_{inlet}\right) - \left(T_{culture} - T_{outlet}\right)}{\ln\left(\frac{T_{culture} - T_{inlet}}{T_{culture} - T_{outlet}}\right)} \quad (13.16)$$

where the left hand side of the equation represents the heat flow gained by the cooling water passing through the internal side of the heat exchanger, and the right hand side represents the heat lost by the culture and transferred to the cooling water. U is the global heat exchanger coefficient (W m^{-2} °C^{-1}) and A is the external surface of the heat exchanger.

d. Scale-Up of Flat Panels

According to the conceptual scheme of Fig. 13.1, the scale-up of the number of flat panel modules for the second step of H_2 production, is based on the M Tn $year^{-1}$ produced in the scale up performed for the first step (biomass production). Thus, the daily M/365 tonnes of biomass produced in the open RW must be re-suspended in the proper medium so that the resulting biomass concentration is over 1 g L^{-1} (i.e., sulphate free-Tris-acetate-phosphate medium (TPA-S) for *C. reinhardtii*; Nitrogen free-Allen-Arnon medium (and no aeration) for the cyanobacteria *Anabaena variabilis*). This dense culture (about 1 g L^{-1}), along with the large surface to volume ratio (optical path of about 3−7 cm) would allow a good use of the solar radiation. This means that the volume of flat panel reactor (m^3) should be about 2.74·M. By taking into account that the volume of one module is 0.1875 m^3 (2.5 m length, 1.5 m high, 0.05 m width), the number of modules needed for culturing the daily biomass produced in the first step is 14.6M. (~15·M).

Bearing in mind that the H_2 production phase last about 4 days in the case of *C. reinhardtii*, and 7 days in the case of cyanobacteria or PNS bacteria, the total amount of modules needed are $4 \times 14.6M$ or $7 \times 14.6M$ (rounding up to 60·M and 100·M respectively). Finally, the land demand required can be estimated by using, as rule of thumb, that the distance between a row of modules and others should be about 0-75-1.00 m.

Note that the use of O_2-free aeration for flat panel reactors, according to the scheme shown in Fig. 13.1, is restricted to the H_2 production by using green microalgae that requires anoxygenic conditions in the second step, i.e., the absence of oxygen from the algal environment. Green algae use the iron [Fe-Fe]-hydrogenase that catalyzes both the production and the consumption of hydrogen through the reversible reaction:

$$2H^+ + 2e^- \leftrightarrow H_2$$

The rate at which the [Fe-Fe]-hydrogenase catalyzes the production of H_2 decreases significantly with increasing partial pressure of H_2, and hence the need of removing the dissolved H_2 by bubbling a stream of O_2-free gas and to maintain a slightly negative pressure (about −4kPa). On the other hand, aerated flat panel technology is not the technology of choice when using cyanobacteria or PNS bacteria in the H_2 production step. Cyanobacteria use either [Ni-Fe]-hydrogenase or nitrogenase (the latter is the enzyme used by PNS bacteria) and both, nitrogen-fixing cyanobacteria and PNS bacteria, in order to produce hydrogen require the absence of nitrogen sources (N_2, NO_3^- or NH_4^+) in addition to anaerobic conditions. Therefore, since in the flat panel technology is mixed by a O_2-free air stream to keep the proper fluid dynamics conditions, the presence of N_2 would inhibit the nitrogenase (if using PNS bacteria), or both [Ni-Fe]-hydrogenase or nitrogenase, depending on the cyanobacterium used in the second step. In the case of a flat panel with internal channels through which the culture is circulated by means of a centrifugal pump, it would be possible the use of cyanobacteria or PNS bacteria in them, as is done with the tubular reactors.

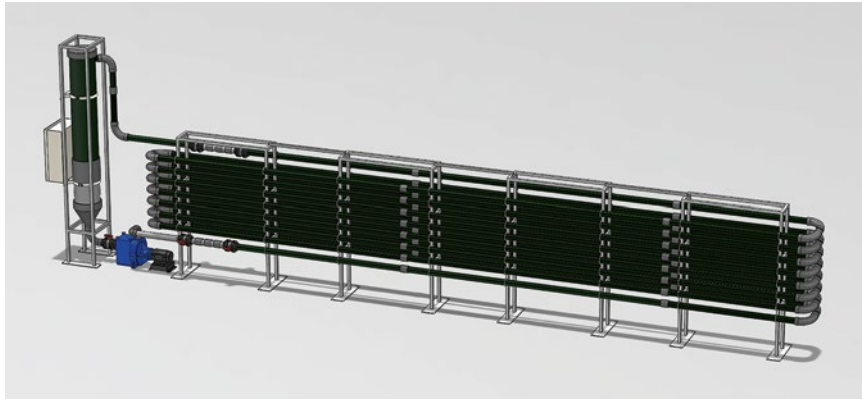

Fig. 13.5. Fence-type tubular photobioreactor.

2. *Tubular Photobioreactors*

Tubular photobioreactors are the most widely used closed systems for the production of microalgae. They consist of a solar collector made of tubes, a degasser unit which usually is a bubble column and a pump for the culture impulsion. A conceptual fence configuration tubular photobioreactor, as those existing in authors' facilities, is shown in Fig. 13.5.

The pump circulates the culture through the solar collector tubing where most of the photosynthesis, or the photofermentative process, occurs. The H_2 produced by photofermentation or photosynthesis is accumulated in the broth (as well as pure H_2 bubbles in the upper part of the tube when the dissolved H_2 concentration exceeds the saturation value) until the fluid returns to the degasser zone (bubble column), where the accumulated hydrogen is stripped by a counter current O_2-free airflow. A gas-liquid separator in the upper part of the bubble column prevents the H_2 bubbles from being recirculated into the solar collector. The major drawback of this technology is the high power consumption used for the impulsion of the liquid through the tube, roughly 500 W m^{-3} for the pump-driven fence configuration (Acién-Fernández et al. 2012). The solar loop is designed to be efficient in collecting the solar radiation and in promoting the light dilution effect, to minimize the resistance to flow and to occupy as little land as possible. Similarly to the flat panels, the diameter of the solar tubing is selected so that the volume of the dark zone (i.e., the zone with light intensity below saturation) is kept to a minimum. Also, the movement of fluid between the light and the dark zones in the solar collector should be rapid enough to prevent an excessive residence time of any element of fluid in the dark zone. Increasing the culture velocity in order to enhance the turbulent mixing (and therefore the light to dark cycle frequencies) and reducing the mixing time appear to be crucial in the photobioreactor scale-up for the hydrogen production stage (Oncel and Sabankay 2012). The length of the tube is limited by the H_2 build-up. As a rule of thumb, the maximum tube length is determined by the maximum dissolved hydrogen that the specific strain can withstand with an acceptable drop in the H_2 production rate. The H_2 stripping capacity of the culture broth is a key factor for designing a tubular reactor for hydrogen production. Increasing the gas phase to the liquid phase by a factor of 4 resulted in a 100 % increase in the H_2 output (Giannelli and Torzillo 2012). These findings are important for a rational design of PBR. However, in the case of the tubular PBR characterized by perfect plug flow behaviour inside the tubes, the increase of the liquid

free surface in the headspace of the degasser has little impact on the gas removal due to the extremely high ratio between the residence time inside the tube circuit compared to that in the degasser. Increasing the flow rate can help to reduce both the mixing and the residence time, thus helping to reduce the contact between the hydrogen gas and the culture. However, replacing the curves with proper designed manifolds conveying the gas toward the degasser could be the best solution to the gas removal problem in a tubular rector (Giannelli and Torzillo 2012). Therefore these reactors are usually modular. The relevant design aspects are discussed next.

a. The Liquid Velocity and Length of the Solar Tube

The design of tubular photobioreactor must guarantee that the flow in the solar tube is turbulent (i.e., Reynolds number should exceed 10,000) so that the cells do not stagnate in the dark interior of the tube. At the same time, the dimensions of the fluid micro eddies should always exceed those of the algal cells; so that turbulence-associated damage is avoided (Acién-Fernández et al. 2001; Camacho et al. 2001). The need to control eddy size places an upper limit on the flow rate through the solar tubing. The length scale of the microeddies may be estimated by applying Kolmogorof's theory of local isotropic turbulence (Kawase and Moo-Young 1990):

$$\lambda = \left(\frac{\mu_L}{\rho}\right)^{3/4} \xi^{-1/4} \tag{13.17}$$

Where λ is the microeddy length, ξ is the energy dissipation per unit mass, μ_L is the viscosity of the fluid, and ρ is the fluid density. The specific energy dissipation rate within the tube depends on the pressure drop and the liquid velocity, U_L,

$$\xi = \frac{2C_f U_L^3}{d_t} \tag{13.18}$$

Where C_f is the Fanning friction factor that can be estimated by using the Blausius equation (Eq. 13.19). Thus, for any selected strain the cell size is known. Using this size as the microeddie length, allows calculating the maximum energy dissipation rate per unit mass (Eq. 13.15), and from this, the maximum liquid velocity, U_l, that makes the microeddie length similar to cell size (Eq. 13.18).

$$C_f = 0.0791 Re^{-0.25} \tag{13.19}$$

Another restriction on the design of the solar collector is imposed by the acceptable upper limit on the concentration of dissolved hydrogen. The length of the solar collector must not be long enough as to achieve an inhibiting hydrogen concentration in the culture. The maximum length, L, is a function of the liquid velocity, dissolved hydrogen concentration and the hydrogen production rate, r_{H2}, and can be calculated as follows:

$$L = \frac{U_L\left(\left[H_2\right]_{out} - \left[H_2\right]_{in}\right)}{r_{H2}} \tag{13.20}$$

Where U_L is the liquid velocity (ratio between the liquid flow rate and the cross sectional area of the tube). Note that U_L is always lower than the maximum velocity imposed by microeddies length. $[H_2]_{in}$ is the hydrogen concentration at the beginning of the solar collector (i.e., the saturation value when the fluid is in equilibrium with the atmosphere), $[H_2]_{out}$, is the hydrogen concentration at the outlet of the solar collector (i.e., maximum acceptable value that does not inhibit hydrogen production), and r_{H2} is the volumetric rate of hydrogen generation reported for the strain in well-controlled laboratory experiments. If the culture is circulated by pumps (fence type configuration), the type and power of the pump determines the liquid velocity. The above Eqs. (13.17), (13.18), (13.19) and (13.20) can also be applied for alveolar flat panel reactors.

Considering the reported data of hydrogen production rates it is possible to determine the maximal length of tubular photobioreactors as a function of the tolerable hydrogen concentration at the beginning and end of the loop. Assuming that the hydrogen production rate is not inhibited at concentrations close to saturation with pure hydrogen, this value can be used for the H_2 concentration at the end of the loop i.e., this is a scenario in which no H_2 bubbles are produced within the tube circuit. For the concentration at the beginning of the loop, a 40 % of the saturation level with pure hydrogen is accepted. The higher the initial hydrogen concentration is, the shorter the loop has to be to prevent oversaturation. On the other hand, a high hydrogen concentration at the beginning of the loop, and hence in the degasser, implies a high driving force for the desorption process thus a lower mass transfer capacity requirement. The mass transfer capacity needed to achieve a stable operation of the system can be calculated from these values if the volumes of the total reactor and of mass transfer unit (V_{mt}) are known. As a rule of thumb, we can take V_{mt} as a 10 % of total tubular photobioreactor volume.

b. Combining Flow and Gas-Liquid Mass Transfer Within the Tube

In the previous scenario, we have assumed that the dissolved hydrogen concentration does not surpass the saturation level in any point of the loop. It is also possible to design for a situation in which the level of dissolved hydrogen be over the saturation value in a part or in the whole loop, giving rise to coexisting gas and liquid phases in the loop. This is highly likely, above all, when working with PNS bacteria because these microorganisms have H_2 production rates substantially higher than rates green algae have. Design of tubular photobioreactors in this scenario must also consider gas-liquid mass transfer and hydrodynamics within the tube. By applying mass balances to the different zones of the tube circuit for which the fluid-dynamic conditions remain constant, the hydrogen transfer between the liquid and gas phase can be modelled. For the liquid phase, the changes in concentrations of dissolved hydrogen along the circuit can be related to the gas-liquid mass transfer rates and the generation rates by mass balances as follows:

$$Q_L\, d\left[H_2\right] = K_l a_{H_2}\left(\left[H_2\right]^* - \left[H_2\right]\right) S dx + r_{H_2}\left(1-\varepsilon\right) S dx \tag{13.21}$$

In this equation, $K_l a_{H2}$ is the volumetric gas-liquid mass transfer coefficient for hydrogen in the solar collector (i.e., within the tube circuit), dx is the differential distance along the direction of flow in the solar tube, $[H_2]$ is the liquid phase concentration of hydrogen, ε is the gas holdup; S is the cross-sectional area of the tube; r_{H2} is the volumetric generation of hydrogen and Q_L is the volumetric flow rate of the liquid. Note that the concentration values marked with an asterisk correspond to the equilibrium concentration, i.e., the maximum possible liquid-phase concentration of hydrogen in contact with the gas phase of a given composition. This term only exists if there is a gas phase from which mass is transferred. The gas phase exists if the culture becomes oversaturated (pure hydrogen bubbles) or gas is artificially injected into the tubes.

As for the liquid phase, a component mass balance can be established also for the gas; hence,

$$dF_{H_2} = -K_l a_{H2}\left(\left[H_2\right]^* - \left[H_2\right]\right) S dx \tag{13.22}$$

Here F_{H2} is the molar flow rate of the hydrogen in the gas phase. Note that because of the change in molar flow rate, the volumetric flow rate of the gas phase may change along the tube. The equilibrium concentrations of the hydrogen in the liquid can be calculated by using the Henry's law:

$$\left[H_2\right]^* = H_{H_2} P_{H_2} = H_{H_2}\left(P_T - P_v\right) \tag{13.23}$$

where H_{H2} is the Henry's constant for hydrogen, P_{H2} is the partial pressure of hydrogen in the gas phase existing in the upper part of the tube (i.e., roughly 1 atm, because gas

phase is almost pure hydrogen); the partial pressures can be calculated knowing the total pressure (P_T) and the vapour pressure (P_v). The previous equations and the initial conditions, allow numerical integration and consequently, the determination of the H_2 axial profiles in the liquid phase and the molar flow rates of H_2 in the gas phase. The model is simple and can be adapted to any photobioreactor and H_2 producing strain in the second phase (note the same rationale and Eqs. (13.21), (13.22) and (13.23) can be used for alveolar flat pannel reactors). Moreover, since the model can simulate the H_2 profile along the tube as a function of the tube length and operational variables, it would allow the rational design and scale-up of tubular PBR for H_2 production.

c. Hydrogen Removal and Temperature Control

Once the solar collector has been designed, it is necessary to calculate the degasser unit used for the removal of hydrogen and temperature control. For this purpose the use of bubble columns (generally used in the fence configuration reactor, Fig. 13.5) is preferred because these systems are simple, well-known and widely used at industrial scale. The mass transfer coefficient can be calculated as a function of O_2-free aeration rate (Eqs. 13.13 and 13.14) and from this the volume of bubble column required to remove the hydrogen is calculated as:

$$V = \frac{Q_L\left([H_2]_{out} - [H_2]_{in}\right)}{K_1 a_1 \bullet \left(\left[H_2^*\right] - [H_2]\right)(1-\varepsilon)} \qquad (13.24)$$

where Q_L is the liquid flow rate entering to the bubble column, $[H_2]_{in}$ is the hydrogen concentration at the inlet of the bubble column, $[H_2]_{out}$ is the hydrogen concentration at the outlet of the bubble column, $K_L a_L$ is the volumetric mass transfer coefficient for the bubble column, and ($[H_2]$*-$[H_2]$) is the driving force for the transport of hydrogen from the liquid to the gas phase, calculated as the logarithmic mean of the concentration difference at the inlet and the outlet. To avoid the recirculation of bubbles from the bubble column to the solar collector, the superficial liquid velocity downstream must be lower than the velocity of the rising bubbles, U_b of the O_2-free stream. Thus, the minimum diameter of bubble column, *dc*, can be calculated (Eq. 13.25), as well as the minimum column height, *hc*, (Eq. 13.26).

$$dc = \sqrt{\frac{4Q_L}{\pi U_b}} \qquad (13.25)$$

$$hc = \frac{4V}{\pi dc^2} \qquad (13.26)$$

The heat transfer equipment must be designed analogously to mass transfer. The equipment must be able to remove the heat absorbed by radiation. This is a function of the solar radiation received by the solar collector, *Qrad*, and the thermal absorptivity of the culture, a_{rad}. Finally, the area of heat exchanger necessary, $A_{exchanger}$ is calculated as a function of the overall heat transfer coefficient, $U_{exchanger}$, and the temperature of cooling water by:

$$A_{exchanger} = \frac{Q_{rad} a_{rad}}{U_{exchanger}\left(T_{culture} - T_{water}\right)} \qquad (13.27)$$

d. Examples of Pilot Scale (>50 L) Sealed PBR for H_2 Production

Although algal H_2 production has been extensively investigated, there are almost no publications on the subject carried out with PBR volumes anything beyond lab-scale. Nonetheless, some publications have started to appear recently with the objective of assessing the production of H_2 in tubular reactors with volume capacities over 50 L using sunlight.

In this sense, Torzillo and co-workers (Scoma et al. 2012) built a 50 L horizontal tubular PBR for producing H_2 with the microalga *Chlamydomonas reinhardtii*. The device was made up of ten parallel glass tubes connected by PVC U-bends (Fig. 13.6). The illuminated area was 1.5 m^2 with a surface-to-volume ratio of 30.5 m^{-1}.

Fig. 13.6. Overview of the 50-L horizontal tubular photobioreactor used for outdoor experiments with *C. reinhardtii*. *Inset*: details of the PVC pump and the degasser (Courtesy of Dr. G. Torzillo, ISE, CNR, Florence, Italy).

The circulation of the fluid within the loop was done with a PVC centrifugal pump with three stainless-steel flat blades placed at an angle of 120º with respect to each other on the propeller shaft. It is interesting to note that the distance between the blades and the box of the rotor is 0.5 cm while the height of the casing is 6.5 cm (see detail in Fig. 13.6). This pump provides adequate fluid dynamics, liquid velocity (range 0.2–0.5 m s^{-1} and mixing time (around 1 min). At the end of the loop (with a total length of 23 m) the culture flows through a 2.2 L degasser (PVC tube, 10 cm internal diameter and 28 cm height). The degasser contains several hose fittings to feed culture medium, flushing gas, and for the withdrawal of culture and gas samples.

During the hydrogen production phase, the headspace of the PBR (i.e., the volume above the culture level) was about 0.2 L (0.4 % of the total volume) and the degasser was flushed with a N_2 gas stream. In our opinion, the free G-L surface in the degasser is very little and so will be the mass transfer capacity of this unit; nonetheless the experiment was performed with a partial vacuum of −4.03 kPa to facilitate the degassing of the dissolved H_2 entering the degasser. The maximum H_2 production rate reported was 0.3 ml L^{-1} h^{-1}, production that was 18 % lower than that obtained with the same microalga in 1 L flat panel reactor. The major differences are in the mixing time (15.5 s) in lab-scale *vs*. 60 s in the 50 L reactor, and in the illumination pattern (both sides illuminated in the 1 L flat reactor while in the 50 L outdoor reactor about a 30 % of the culture is permanently in dark). The illumination and mixing degree have both been proved to be key features to take into account in the scale-up of the H_2 production phase; although as commented before, care must be taken with the potential damage of cells caused by an excessive turbulence level (Oncel and Sabankay 2012). Therefore, the scaling up of this tubular configuration has serious difficulties since the increase of liquid velocity needed to achieve the proper light-dark cycle frequencies may conflict with the cell damage that this can cause.

The same reactor has also been used by Adessi et al. (2012) for H_2 production by the purple non-sulphur bacterium *Rhodopseudomonas palustris*. The average H_2 production rate was 10.7 ml L^{-1} h^{-1} with a

reported maximum of 27.2 ml L^{-1} h^{-1}. These productivities were two orders of magnitude higher that that obtained with *C. reinhardtii* with the same reactor and similar environmental conditions. A micro sensor for measuring the dissolved H_2 concentration in the range 0.0–1.5 mg L^{-1} (i.e., 0.0–0.75 mM) revealed that the elapsed time from the sunrise until dissolved hydrogen appeared in the culture was about 1.3 h and that H_2 gas was effectively collected between 11:00 and 19:00 h local time (Adessi et al. 2012). The light to H_2 conversion efficiency with the PNS bacteria was 0.63 *vs.* the 0.21 % for *C. reinhardtii*. This shows how the processes based on PNS bacteria are more promising than those using green algae.

A 80 L tubular reactor for the H_2 production with the PNS bacterium *Rhodobacter capsulatus* by the photofermentation of thick juice effluents was designed by Boran et al. (2010, 2012). The reactor was placed with an inclination of 10º. This reactor is conceptually similar to the near horizontal tubular reactor designed by Tredici et al. (1998). The tubular reactor consisted of 9 tubes, 6 cm diameter and 2.35 m length. The total illuminated surface was 2 m^2 and the occupied ground area was 2.88 m^2. During the H_2 production phase, the culture was bubbled with an argon stream. The reactor temperature was kept below 35 °C by internal cooling coils. The culture was carried out in a semicontinuous mode with a dilution rate of 0.11 d^{-1}, trying to maintain cell concentration at around 1 g L^{-1} during the H_2 production phase. The average H_2 production rate was 0.15 mol $H_2 m^{-3}$ h^{-1}during 9 days, obtaining a light conversion efficiency of roughly 0.2 %, and demonstrating that the H_2 yield of the culture (mmol H_2 to cell dry weight ratio) was a potential function of the total light energy, E, received ($W \cdot h\ m^{-2}$), with a 1.4 exponent.

Possibly, the work carried out at the largest scale so far has been performed by Torzillo and co-workers by using a 110 L tubular PBR immersed in a light-scattering nanoparticle suspension (Fig. 13.7) (Giannelli and Torzillo 2012). The PBR was made up of 64 tubes (i.d., 2.75 cm; length 2 m) connected by 64 U-bends, with a total 133 m length. The tubes were immersed in a light scattering suspension of silica nanoparticles that increases the H_2 production rate up to 0.62 ml L^{-1} h^{-1} *vs.* the 0.42 ml L^{-1} h^{-1} achieved without immersing them into the nanoparticles bath (note that these productivities almost doubled those obtained in the 50 L reactor shown in Fig. 13.6). This demonstrates the positive effect of the dilution of light by nanoparticles, which enhances the H_2 production. In our opinion, the drawbacks already existing in the 50 L reactor (Fig. 13.6) are still present in this new design. The degasser again is hardly 2 L volume. During the H_2 production phase, the headspace of the degasser was 0.35 L (i.e., 15 % of the total volume of the degasser). Apparently, the mass transfer capacity of this reactor, similar to the 50 L reactor, is clearly insufficient. The light to H_2 conversion efficiency was only 0.21 %. Ignoring the economical considerations, the new method presented in this design for the dilution of light shows at least two major advancements over the state of the art of sealed PBR for H_2 production: (1) it not only improves the light conversion efficiency, but this new design also allows an efficient way for PBR scaling up by reducing the distance between the tubes, and consequently increasing the number of tubes, without altering the foot print; and (2) it is possible to modify the irradiance impinging on the surface of the tubes by varying the concentration of nanoparticles. This is a significant advantage in outdoor cultures where the intense direct light radiation may cause over saturation with loss of efficiency. With the PBR concept designed by Torzillo´s group, even direct incident sunlight can be diluted to levels of photosynthesis saturation (about 200 μE m^{-2} s^{-1}). Nonetheless, this new PBR design has only been operated so far with artificial light and it needs to be demonstrated operating with sunlight to actually test the above commented advancements.

e. Scale-Up of Tubular PBR

For practical purposes, the scaling up of a tubular photobioreactor requires the scaling

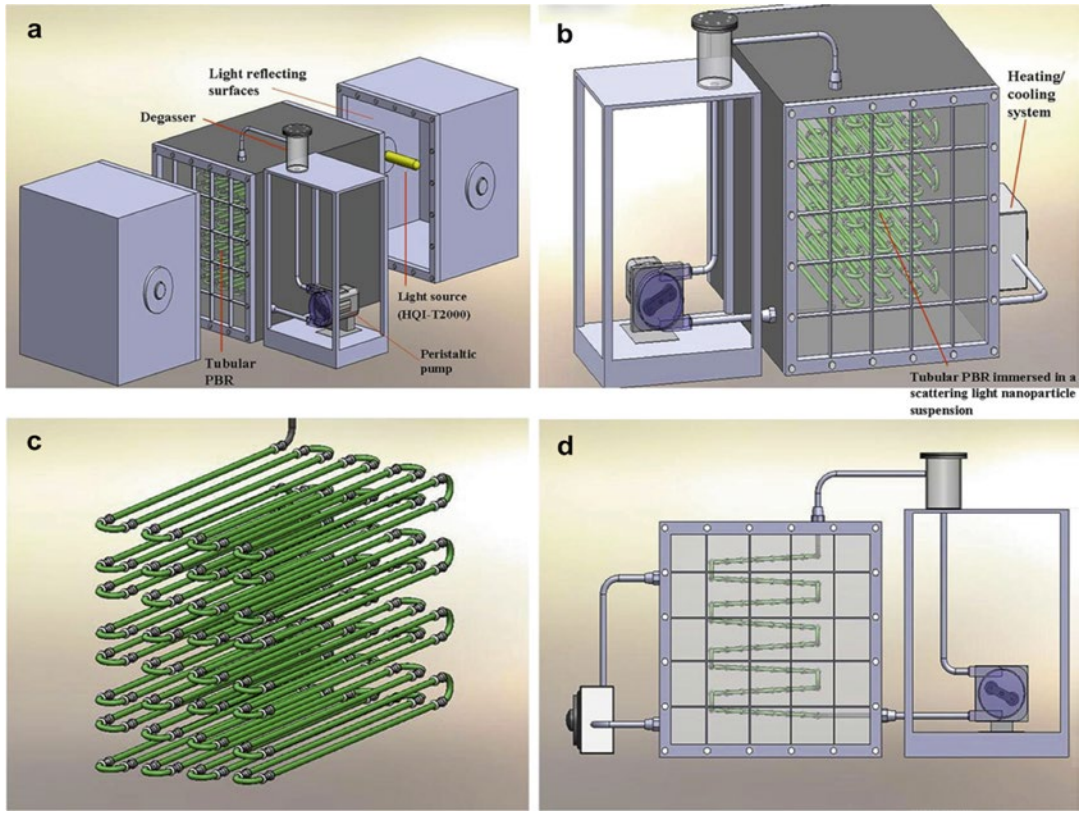

Fig. 13.7. Enclosed tubular photobioreactor used for f H_2 production with *C. reinhardtii* (**a**) general view of the 110-L PBR (**b**) frontal view of the tubular PBR set in a container filled with a light scattering nanoparticle suspension (**c**) detail of the PBR made up eight tube layers and connected each other by U-bends to form a 133 m long circuit (**d**) frontal view of the reactors showing the tube layers with opposite inclination to facilitate culture draining (Photography and description, courtesy of Dr. G. Torzillo, ISE, CNR, Florence, Italy).

up of both the solar receiver and the degasser system (i.e., the bubble column in the case of fence type configuration). Scaling of the degasser does not pose a limitation for any realistic size of the photobioreactor. However, there are limitations in the scaling up of a continuous run solar loop. In principle, the volume of the loop may be increased by increasing the diameter and the length of the tube. In practice, the maximum tube length is limited by gas buildup and the diameter should not exceed 0.10 m (Molina Grima et al. 2000; Brindley et al. 2004). Figure 13.8 shows an industrial size photobioreactor operated in a greenhouse in Almería, Spain, following Eqs. (13.7) to (13.8) and (13.17), (13.18), (13.19), (13.20), (13.21), (13.22), (13.23), (13.24), (13.25), (13.26) and (13.27) (Acién-Fernández et al. 2013). This reactor was scaled up to industrial size with the objective of producing a metabolite associated to growth. The production of biomass involves the removal of O_2 and the supply of CO_2, and therefore there are some differences between Eqs. (13.20), (13.21), (13.22), (13.23) and (13.24) and those shown for O_2 removal and CO_2 supply in Acién-Fernández et al. (2013). This reactor is running in the authors' facilities for producing high value products and may be adapted with some small modifications (head space of the degasser and type of centrifugal pump for liquid impulsion) to produce H_2.

For the scaling up of tubular reactors, first the light availability in PBR location should be calculated according to solar radiation

Fig. 13.8. Photograph of an industrial size fence configuration tubular photobioreactor 30 m^3 plant for the production of lutein from *Scenedesmus almeriensis* Almería. Fundación CAJAMAR (With permission of Fundación CAJAMAR, Almería, SPAIN).

knowledge. Then, simulations should be performed to determine the optimal tube diameter. The selection should be done taking into account the characteristic parameters of the microalga, cyanobacterium or PNS bacterium to be used (μ_{max}, Ik, n, Eq. 13.6). A practical tube diameter range of 6–9 cm is convenient (Brindley et al. 2004). This range allows the reactor operation at the proper fluid-dynamics conditions, promoting adequate light to dark cycle frequencies and a limited energy consumption. According to the target H_2 productivity r_{H2}, the maximum length of the solar collector can calculated with Eq. (13.20). Table 13.2 shows the tube length for a tubular reactor, similar to that presented in Fig. 13.8, for H_2 production in a scenario in which, during the time spent by the culture in the circuit tube no bubbles are generated. The dissolved hydrogen concentration at the beginning of the loop is 40 % of the saturation with pure hydrogen and 100 % saturation at the exit. This means that in the degasser of the tubular system, the counter current O_2-free airflow removes the 60 % of the dissolved hydrogen of the culture, which enters in degasser saturated. As can be seen in Table 13.2, provided that the hydrogen production rate is over 10^{-3} mol L^{-1} h^{-1} the length of the tube needed in order to have the culture hydrogen saturated is in the reasonable range 100–400 m. For lower hydrogen production rates, the culture will never reach saturation and tube length needed is much lower. Table 13.3 shows the tube length needed for the different scenario in which hydrogen bubbles are formed within the tubes (visible in the upper part of the tube), which have to be dragged to the degasser by the culture motion. The calculations have been made considering that the dissolved oxygen concentration at the entrance and exit of the solar collector are 40 % with respect to saturation with pure hydrogen and twice the saturation, respectively. In these conditions there is a large proportion of tube showing bubbles in the upper part. This scenario is more reasonable when using PNS bacteria in the H_2 production step, since their reported H_2 productivities are almost double in comparison with those obtained with green microalgae. Finally, a bubble column can be designed to be coupled to the solar collector to remove hydrogen as well as to control the temperature of the culture, Eqs. (13.24), (13.25), (13.26) and (13.27).

Table 13.2. Permissible length of tubular reactors as a function of hydrogen production rate, r_{H2}, reported.

Productivity (mol/L·h)	Tube length (m)	Volume (L)	Vmt (L)	Kla (1/h)
2.77E-05	19,900	11,820	1,182	0.47
2.00E-03	275	1,752	175	33.62
5.80E-04	949	6,038	604	9.76
1.50E-03	367	2,336	234	25.21
1.68E-03	329	2,091	209	28.17
1.83E-04	3,009	19,144	1,914	3.08
2.01E-05	27,418	174,423	17,442	0.34
2.50E-04	2,203	14,016	1,402	4.20
1.21E-03	454	2,886	289	20.41
5.90E-03	93	594	59	99.18

Values were obtained considering a liquid velocity of 0.3 m/s, and hydrogen dissolved concentrations at the beginning and end of the tube circuit equal to 40 % of saturation with pure hydrogen ($[H_2] = 3.4 \cdot 10^{-4}$ mol/L) and saturation with pure hydrogen ($[H_2]_{sat} = 8.50 \cdot 10^{-4}$ mol/L), respectively
The references for these values are the same as in Table 13.1

Table 13.3. Tube length of tubular photobioreactor as a function of hydrogen production rate values reported.

Productivity (mol/L·h)	Tube length (m)	Volume (L)	Vmt (L)	Kla (1/h)
2.77E-05	53,066	31,519	3,152	0.27
2.00E-03	734	4,672	467	19.61
5.80E-04	2,531	16,101	1,610	5.69
1.50E-03	979	6,229	623	14.71
1.68E-03	876	5,575	558	16.43
1.83E-04	8,025	51,051	5,105	1.79
2.01E-05	73,114	465,129	46,513	0.20
2.50E-04	5,875	37,376	3,738	2.45
1.21E-03	1,210	7,695	770	11.91
5.90E-03	249	1,584	158	57.85

Values obtained considering a liquid velocity of 0.3 m/s, and hydrogen concentrations at the beginning and end of the tube loop equal to 40 % of saturation with pure hydrogen ($[H_2] = 3.4 \cdot 10^{-4}$ mol/L) and double than saturation with pure hydrogen ($2x[H_2]_{sat} = 1.7 \cdot 10^{-3}$ mol/L), respectively

V. Concluding Remarks

This chapter shows the fundamental principles of photobioreactor design to be used in a hypothetical facility (Fig. 13.1) to produce hydrogen from green microalgae, cyanobacteria or PNS bacteria. This has been envisaged from the pioneering work of Melis et al. (2000), showing the possibility to separate the biomass production stage and the H_2 production stage for a culture of *C. reinhardtii*. The challenges associated with the two closed technologies capable of producing H_2were discussed followed with strategies to overcome the major technical issues. The previous experience and tools for the design and scaling up of industrial reactors has been adapted for the photobiological production of hydrogen in completely sealed photobioreactors. However the data available on hydrogen production is scarce for systems over 50 L capacity, and the light to H_2 conversion efficiencies, whatever the route used for producing H_2, are well below 1 %. Therefore the calculations made are subjected to many uncertainties. The majority of data on hydrogen production rate used have been taken from laboratory scale photobioreactors, which rarely exceed the 2 L, given the scarcity of outdoor pilot H_2 production. The length of 9 cm tube needed for the two production scenarios covered in Tables 13.2 (no H_2 bubbles in the tube circuit) and 13.3 (presence

of H_2 bubbles) gives rise to volume reactors able to be fed with the harvested biomass produced, in a first step, in an open raceway facility producing about 2 and 4 tonnes of biomass (d.w) per year, respectively. In brief, photobiological hydrogen production is at an early stage of development that requires much more pilot experience.

Acknowledgements

The authors wish to acknowledge the contribution of all our colleagues of the Marine Microalgae Biotechnology Group of the University of Almería who have worked with us in the design and assessment of photobioreactors in the last 15 years. Special acknowledgement to Cajamar Foundation and the financial support from projects granted by EU (EnerBioAlgae. SOE2/P2/E374. SUDOE INTERREG IVB), Secretatia de Estado de Investigación, Ministerio de Economía y Competitividad (Project DPI2011-27818-C02-01) as well as by FEDER funds, PlanE for microalgae, ACCIONA S.A., ENDESAS.A. and Junta de Andalucía (CVI 131 &173).

References

Acién-Fernández FG, García Camacho F, Sánchez Pérez JA, Fernández Sevilla JM, Molina Grima E (1997) A model for light distribution and average solar irradiance inside outdoor tubular photobioreactors for the microalgal mass culture. Biotechnol Bioeng 55:701–714

Acién-Fernández FG, García Camacho F, Sánchez Pérez JA, Fernández Sevilla JM, Molina Grima E (1998) Modeling of biomass productivity in tubular photobioreactors for microalgal cultures: effects of dilution rate, tube diameter, and solar irradiance. Biotechnol Bioeng 58:605–616

Acién-Fernández FG, Fernández Sevilla JM, Sánchez Perez JA, Molina Grima E, Chisti Y (2001) Airlift-driven external-loop tubular photobioreactors for outdoor production of microalgae: assessment of design and performance. Chem Eng Sci 56:2721–2732

Acién-Fernández FG, Fernández Sevilla JM, Magán JJ, Molina Grima E (2012) Production cost of a real microalgae production plant and strategies to reduce it. Biotechnol Adv 30:1344–1353

Acién-Fernández FG, Fernández Sevilla JM, Molina Grima E (2013) Principles of photobioreactor design. In: Posten C, Walter C (eds) Microalgal biotechnology: potential and production. De Grutier, Göttingen, pp 151–179

Adessi A, Torzillo G, Baccetti E, De Philippis R (2012) Sustained outdoor H_2 production with *Rhodopseudomonas palustris* cultures in a 50 L tubular photobioreactor. Int J Hydrog Energy 37:8840–8849

Akkerman I, Jansen M, Rocha J, Wijjfels RH (2002) Photobiological hydrogen production: photochemical efficiency and bioreactor design. Int J Hydrog Energy 27:1195–1208

Antal T, Krendeleva T, Laurinavichene T, Makarova V, Ghirardi M, Rubin A, Tsygankov AA, Seibert M (2003) The dependence of algal H_2 production on photosystem II and O_2 consumption activities in sulfur-deprived *Chlamydomonas reinhardtii* cells. Biochim Biophys Acta 1607:153–160

Azov Y, Shelef G (1982) Operation of high-rate oxidation ponds: theory and experiments. Water Res 16:1153–1160

Benemann JR (1997) Feasibility analysis of photobiological hydrogen production. Int J Hydrog Energy 228:979–987

Benemann JR (2000) Hydrogen production by microalgae. J Appl Phycol 12:291–300

Berberoglu H, Jay J, Pilon L (2008) Effect of nutrient media on photobiological hydrogen production by *Anabaena variabilis* ATCC 29413. Int J Hydrog Energy 33:1172–1184

Boran E, Özgür E, van der Burg J, Yücel M, Gündüz U, Eroglu I (2010) Biological hydrogen production by *Rhodobacter capsulatus* in solar tubular photo bioreactor. J Clean Prod 18:S29–S35

Boran E, Özgür E, Yücel M, Gündüz U, Eroglu I (2012) Biohydrogen production by *Rhodobacter capsulatus* in solar tubular photobioreactor on thick juice dark fermenter effluent. J Clean Prod 3:150–157

Brindley C, Garcia-Malea MC, Acién-Fernández FG, Fernández Sevilla JM, García Sánchez JL, Molina Grima E (2004) Influence of power supply in the feasibility of *Phaeodactylum tricornutum* cultures. Biotechnol Bioeng 87:723–733

Camacho Rubio F, Molina Grima E, Valdés Sanz F, Andújar Peral JM (1991) Influence of operational and physical variables on interfacial area determination. AIChE J 37:1196–1204

Camacho Rubio F, Acién-Fernández FG, Sánchez Pérez JA, García Camacho F, Molina Grima E (1999)

Prediction of dissolved oxygen and carbon dioxide concentration profiles in tubular photobioreactors for microalgal culture. Biotechnol Bioeng 62:71–86

Camacho FG, Molina Grima EM, Mirón AS, Pascual VG, Chisti Y (2001) Carboxymethyl cellulose protects algal cells against hydrodynamic stress. Enzyme Microb Technol 29:602–610

Chisti Y (2013) Raceways-based production of algal crude oil. In: Posten C, Walter C (eds) Microalgal biotechnology: potential and production. De Grutier, Göttingen, pp 113–146

Chochois V, Dauvillée D, Beyly A, Tolleter D, Cuiné S, Timpano H, Ball S, Cournac L, Peltier G (2009) Hydrogen production in *Chlamydomonas:* photosystem II-dependent and independent pathways differ in their requirement for starch metabolism. Plant Physiol 151:631–640

Das D, Veziroglu TN (2001) Hydrogen production by biological processes: a survey of literature. Int J Hydrog Energy 26:13–28

Das D, Veziroglu TN (2008) Advances in biological hydrogen production processes. Int J Hydrog Energy 33:6046–6057

Doucha J, Livansky K, Kostelnik K (1996) Thin-layer microalgal culture technology. Abstracts of the 7th international conference of applied. Algology, Knysna, South Africa, p 32

Doucha J, Straka F, Lívanský K (2005) Utilization of flue gas for cultivation of microalgae (*Chlorella* sp.) in an outdoor open thin-layer photobioreactor. J Appl Phycol 17:403–412

Eroglu E, Melis A (2011) Photobiological hydrogen production: recent advances and state of the art. Bioresour Technol 102:8403–8413

Florin L, Tsokoglou A, Happe T (2001) A novel type of iron hydrogenase in the green alga *Scenedesmus obliquus* is linked to the photosynthetic electron transport chain. J Biol Chem 276:6125–6132

García Camacho F, Contreras A, Acién-Fernández FG, Fernández JM, Molina Grima E (1999) Use of concentric-tube airlift photobioreactors for microalgal outdoor mass cultures. Enzyme Microb Technol 24:164–172

Giannelli L, Torzillo G (2012) Hydrogen production with the microalga *Chlamydomonas reinhardtii* grown in a compact tubular photobioreactor immersed in a scattering light nanoparticle suspension. Int J Hydrog Energy 37:16951–16961

Giannelli L, Scoma A, Torzillo G (2009) Interplay between light intensity, chlorophyll concentration and culture mixing on the hydrogen production in sulfur-deprived *Chlamydomonas reinhardtii* cultures grown in laboratory photobioreactors. Biotechnol Bioeng 104:76–90

Grobbelaar JU (1994) Turbulence in mass algal cultures and the role of light/dark fluctuations. J Appl Phycol 6:331–335

Hallenbeck PC, Benemann JR (2002) Biological hydrogen production: fundamentals and limiting processes. Int J Hydrog Energy 27:1185–1193

Hallenbeck PC, Abo-Hashesh M, Ghosh D (2012) Strategies for improving biological hydrogen production. Bioresour Technol 110:1–9

Hemshemeier A, Fouchard S, Cournac L, Peltier G, Happe T (2008) Hydrogen production by *Chlamydomonas reinhardtii*: an elaborate interplay of electron sources and sinks. Planta 227:397–407

Hu Q, Guterman H, Richmond A (1996) A flat inclined modular photobioreactor for outdoor mass cultivation of photoautotrophs. Biotechnol Bioeng 51:51–60

Incropera FP, Thomas JF (1978) A model for solar radiation conversion to algae in a shallow pond. Sol Energy 20:157–165

James SC, Boriah V (2010) Modeling algae growth in an open-channel raceway. J Comp Biol 17: 895–906

Jiménez C, Cossío BR, Niell FX (2003) Relationship between physicochemical variables and productivity in open ponds for the production of *Spirulina*: a predictive model of algal yield. Aquaculture 221:331–345

Kapdan IK, Kargi F (2006) Bio-hydrogen production from waste materials. Enzyme Microb Technol 38:569–582

Kawase Y, Moo-Young M (1990) Mathematical models for design of bioreactors: applications of Kolmogoroff's theory of isotropic turbulence. Chem Eng J 43:B19–B41

Laurinavichene TV, Fedorov AS, Ghirardi ML, Seibert M, Tsygankov AA (2006) Demonstration of sustained hydrogen production by immobilized, sulfur-deprived *Chlamydomonas reinhardtii* cells. Int J Hydrog Energy 5:659–667

Laws EA, Taguchi S, Hirata J, Pang L (1986) High algal production rates achieved in a shallow outdoor flume. Biotechnol Bioeng 28:191–197

Lee YK, Low CS (1992) Productivity of outdoor algal cultures in enclosed tubular photobioreactor. Biotechnol Bioeng 40:1119–1122

Levin DB, Pitt L, Love M (2004) Biohydrogen production: prospects and limitations to practical application. Int J Hydrog Energy 29:173–185

Markov SA, Thomas AD, Bazin MJ, Hall DO (1997) Photoproduction of hydrogen by cyanobacteria under partial vacuum in batch culture or in a photobioreactor. Int J Hydrog Energy 22:521–524

Melis A, Zhang LP, Forestier M, Ghirardi ML, Seibert M (2000) Sustained photobiological hydrogen gas production upon reversible inactivation of oxygen

evolution in the green alga *Chlamydomonas reinhardtii*. Plant Physiol 122:127–135

Moheimani NR, Borowitzka MA (2007) Limits to productivity of the alga *Pleurochrysis carterae* (haptophyta) grown in outdoor raceway ponds. Biotechnol Bioeng 96:27–36

Molina Grima E (1999) Microalgae, mass culture methods. In: Flickinger MC, Dew SW (eds) Encyclopedia of bioprocess technology: fermentation. Biocatalysis and bioseparations. Wiley, New York, pp 1753–1769

Molina Grima E, Garcia Camacho F, Sanchez Perez JA, Fernandez Sevilla JM, Acién-Fernández FG, Contreras Gomez A (1994) A mathematical model of microalgal growth in light-limited chemostat culture. J Chem Technol Biotechnol 61:167–173

Molina Grima E, Fernández Sevilla JM, Sánchez Pérez JA, García Camacho F (1996) A study on simultaneous photolimitation and photoinhibition in dense microalgal cultures taking into account incident and averaged irradiances. J Biotechnol 45:59–69

Molina Grima E, Acién-Fernández FG, García Camacho F, Camacho Rubio F, Chisti Y (2000) Scale-up of tubular photobioreactors. J Appl Phycol 12:355–368

Molina Grima E, Fernández Sevilla JM, Acién-Fernández FG (2010) Microalgae, mass culture methods. In: Flickinger MC (ed) Encyclopedia of industrial biotechnology: bioprocess, bioseparation, and cell technology. Willey, New York, pp 1–24

Oncel S, Sabankay M (2012) Microalgal biohydrogen production considering light energy and mixing time as the two key features for scale-up. Bioresour Technol 12:228–234

Oswald WJ (1988) Large scale algal culture systems. In: Borowitzka MA, Borowitzka LJ (eds) Microalgal biotechnology. Cambridge University Press, Cambridge, MA, pp 305–328

Oswald WJ, Golueke CG (1968) Large scale production of microalgae. In: Mateless RI, Tannenbaum SR (eds) Single cell protein. MIT Press, Cambridge, MA, pp 271–305

Park JBK, Craggs RJ (2010) Wastewater treatment and algal production in high rate algal ponds with carbon dioxide addition. Water Sci Technol 61:633–639

Park JBK, Craggs RJ, Shilton AN (2011) Wastewater treatment high rate algal ponds for biofuel production. Bioresour Technol 102:35–42

Phillips JN, Myers J (1954) Growth rate of Chlorella in flashing light. Plant Physiol 29:152–161

Pinto FA, Troshina LO, Lindblad P (2002) A brief look at three decades of research on cyanobacterial hydrogen evolution. Int J Hydrog Energy 27:1209–1215

Posewitz M, Smolinski S, Kanakagiri S, Melis A, Seibert M (2004) Hydrogen photoproduction is attenuated by disruption of an isoamylase gene in *Chlamydomonas reinhardtii*. Plant Cell 16:2151–2163

Posten C (2009) Design principles of photobioreactors for cultivation of microalgae. Eng Life Sci 9:165–177

Prince RC, Kheshgi HS (2005) The photobiological production of hydrogen: potential efficiency and effectiveness as a renewable fuel. Criti Rev Microbiol 31:9–31

Pulz O, Scheibenbogen K (1998) Photobioreactors: design and performance with respect to light energy input. Adv Biochem Eng Biotechnol 59:123–152

Putt R, Singh M, Chinnasamy S, Das KC (2011) An efficient system for carbonation of high-rate algae pond water to enhance CO_2 mass transfer. Bioresour Technol 102:3240–3245

Qiang H, Richmond A (1996) Productivity and photosynthetic efficiency of *Spirulina platensis* as affected by light intensity, algal density and rate of mixing in a flat plate photobioreactor. J Appl Phycol 8:139–145

Qiang H, Guterman H, Richmond A (1996) A flat inclined modular photobioreactor for outdoor mass cultivation of photoautotrophs. Biotechnol Bioeng 51:51–60

Rodolfi L, Chini Zittelli G, Bassi N, Padovani G, Biondi N, Bonini G, Tredici MR (2009) Microalgae for oil: strain selection, induction of lipid synthesis and outdoor mass cultivation in a low-cost photobioreactor. Biotechnol Bioeng 102:100–112

Rupprecht J, Hankamer B, Mussgnug J, Ananyev G, Dismukes C, Kruse O (2006) Perspectives and advances of biological H_2 production in microorganisms. Appl Microbiol Biotechnol 72:442–449

Sasikala K, Ramana CV, Rao PR (1991) Environmental regulation for optimal biomass yield and photoproduction of hydrogen by *Rhodobacter sphaeroides* O.U. 001. Int J Hydrog Energy 16:597–601

Scoma A, Giannelli L, Faraloni C, Torzillo G (2012) Outdoor H_2 production in a 50-L tubular photobioreactor by means of a sulfur-deprived culture of the microalga *Chlamydomonas reinhardtii*. J Biotechnol 157:620–627

Sierra E, Acién-Fernández FG, Fernández JM, García JL, González C, Molina Grima E (2008) Characterization of a flat plate photobioreactor for the production of microalgae. Chem Eng J 138:136–147

Sveshnikov DA, Sveshnikova NV, Rao KK, Hall DO (1997) Hydrogen metabolism of mutant forms of *Anabaena variabilis* in continuous cultures and under nutritional stress. FEMS Microbiol Lett 147:297–301

Terry KL (1986) Photosynthesis in modulated light: quantitative dependence of photosynthetic enhancement on flashing rate. Biotechnol Bioeng 28:988–995

Tredici MR, Chini Zittelli C, Benemann JR (1998) A tubular internal gas exchange photobioreactor for biological hydrogen production. In: Zaborsky OR (ed) BioHydrogen. Plenum Press, New York, pp 391–402

Tsygankov AA, Hall DO, Liu J, Rao KK (1998) An automated helical photobioreactor incorporating cyanobacteria for continuous hydrogen production. In: Zaborsky OR (ed) BioHydrogen. Plenum Press, New York, pp 431–440

Tsygankov AA, Borodin VB, Rao KK, Hall DO (1999) H_2 photoproduction by batch culture of *Anabaena variabilis* ATCC 29413 and its mutant PK84 in a photobioreactor. Biotechnol Bioeng 64:709–715

Tsygankov AA, Fedorov AS, Kosourov SN, Rao KK (2002) Hydrogen production by cyanobacteria in an automated outdoor photobioreactor under aerobic conditions. Biotechnol Bioeng 80:777–785

Verlaan P, Van Eijs AMM, Tramper J, Van't Riet K (1989) Estimation of axial dispersion in individual sections of an airlift-loop reactor. Chem Eng Sci 44:1139–1146

Vonshak A (1997) *Spirulina*: growth, physiology and biochemistry. In: Vonhask A (ed) *Spirulina platensis* (*Arthrospira*): physiology, cell-biology and biotechnology. Taylor & Francis, London, pp 43–65

Weissman JC, Goebel RP (1987) Design and analysis of microalgal open pond systems for the purpose of producing fuels: A subcontract report. United States: SERI/STR-231-2840

Weissman JC, Goebel RP, Benemann JR (1988) Photobioreactor design: mixing, carbon utilization, and oxygen accumulation. Biotechnol Bioeng 31:336–344

Winkler M, Hemschemeier A, Gotor C, Melis A, Happe T (2002) [Fe]-hydrogenases in green algae: photofermentation and hydrogen evolution under sulfur deprivation. Int J Hydrog Energy 27:1431–1439

Winkler M, Kuhlgert S, Hippler M, Happe T (2009) Characterization of the key step for light-driven hydrogen evolution in green algae. J Biol Chem 284:36620–36627

Wykoff DD, Davies JP, Melis A, Grossman AR (1998) The regulation of photosynthetic electron transport during nutrient deprivation in *Chlamydomonas reinhardtii*. Plant Physiol 117:129–135

Yoon JH, Shin JH, Kim MS, Sim SJ, Park TH (2006) Evaluation of conversion efficiency of light to hydrogen energy by *Anabaena variabilis*. Int J Hydrog Energy 31:721–727